MIT Open Access Articles

Flexible cylinder flow-induced vibration

Massachusetts Institute of Technology

Flexible cylinder flow-induced vibration F

iD Leixin Ma (马磊鑫), Ke Lin (林柯), iD Dixia Fan (范迪夏), et al.

COLLECTIONS

F   This paper was selected as Featured

View Online   Export Citation   CrossMark

Flexible cylinder flow-induced vibration Ⓕ

View Online   Export Citation   CrossMark

Leixin Ma (马磊鑫),[1] ⓘD Ke Lin (林柯),[2,a] Dixia Fan (范迪夏),[1,3,4,5,a] ⓘD Jiasong Wang (王嘉松),[2] ⓘD
and Michael S. Triantafyllou[1] ⓘD

AFFILIATIONS

[1]Department of Mechanical Engineering, Massachusetts Institute Technology, Cambridge, Massachusetts 02139, USA
[2]Department of Engineering Mechanics, School of Naval Architecture, Ocean and Civil Engineering, Shanghai Jiao Tong University, Shanghai 200240, China
[3]Department of Mechanical and Materials Engineering, Queen's University, Kingston, Ontario K7M 3N9, Canada
[4]School of Engineering, Westlake University, Hangzhou, Zhejiang 310024, China
[5]MIT Sea Grant College Program, Massachusetts Institute of Technology, Cambridge, Massachusetts 02139, USA

[a]Authors to whom correspondence should be addressed: dixia.fan@queensu.ca and linke.sjtu@sjtu.edu.cn

ABSTRACT

In this paper, we conducted a selective review on the recent progress in physics insight and modeling of flexible cylinder flow-induced vibrations (FIVs). FIVs of circular cylinders include vortex-induced vibrations (VIVs) and wake-induced vibrations (WIVs), and they have been the center of the fluid-structure interaction (FSI) research in the past several decades due to the rich physics and the engineering significance. First, we summarized the new understanding of the structural response, hydrodynamics, and the impact of key structural properties for both the isolated and multiple circular cylinders. The complex FSI phenomena observed in experiments and numerical simulations are explained carefully via the analysis of the vortical wake topology. Following up with several critical future questions to address, we discussed the advancement of the artificial intelligent and machine learning (AI/ML) techniques in improving both the understanding and modeling of flexible cylinder FIVs. Though in the early stages, several AL/ML techniques have shown success, including auto-identification of key VIV features, physics-informed neural network in solving inverse problems, Gaussian process regression for automatic and adaptive VIV experiments, and multi-fidelity modeling in improving the prediction accuracy and quantifying the prediction uncertainties. These preliminary yet promising results have demonstrated both the opportunities and challenges for understanding and modeling of flexible cylinder FIVs in today's big data era.

I. INTRODUCTION

Structures like offshore pipelines are subject to flow-induced vibrations (FIVs) under the external fluid flows, shown in Fig. 1. Such a periodic fluid-structure interaction (FSI) process will increase the fatigue damage of the structure, which is difficult to predict. Based on the research over the past several decades, excellent reviews were written.[1–11] However, the problems of bluff body FIVs, especially for flexible cylinders, are by no means solved and fully understood. The present paper aims to complement the previous reviews and focuses on the new advancement in physics insight and modeling of the flexible cylinder vortex-induced vibrations (VIVs) and wake-induced vibrations (WIVs), given the light of more recent developments.

Over the past decade, several well-controlled lab experiments, large-scale field observations, and high-fidelity computational fluid dynamics (CFD) simulations have been conducted to understand FIVs of flexible cylinders with different structural configurations and various environmental conditions. Compared to rigid cylinder FIVs,[12] flexible cylinders exhibit more complicated distributed structural vibrations and vortical wake patterns. Various structural vibration patterns have been observed under different experimental conditions. For instance, it was found that the response in the mildly sheared flow was more likely to show multiple-mode, non-"lock-in" behavior than that in highly sheared conditions.[13–15] The VIV response for small-aspect-ratio flexible cylinders in uniform flow was dominated by standing waves, while significant traveling wave responses[16–18] were observed for large-scale field experiments.[19] The cylinders at a similar level of $m^*\zeta$ could exhibit very different response amplitudes.[20] These new phenomena encourage researchers to conduct more systematic investigations to reveal the fundamental physical mechanism behind this FSI process.

Various numerical models have been proposed to simulate this nonlinear FSI problem.[5] High-fidelity CFD tools have shown great
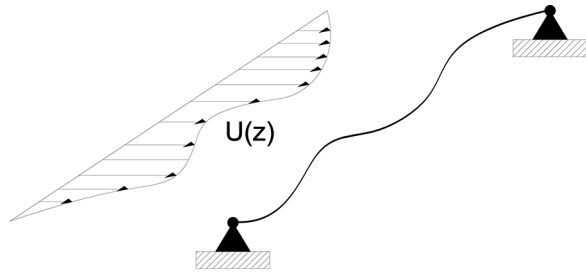
FIG. 1. A sketch of the vortex induced vibrations of flexible cylinders within a non-uniform flow profile.

promise to shed light, especially on the vortical wake topology.[21] However, their computational cost is still too high for industrial applications. Therefore, empirical modeling is still used as the leading toolkit for engineering applications for its efficiency.[22–24] The VIV fluid forcing on the slender structures is often modeled as a nonlinear function of structural vibration amplitude, frequency, and current profile conditions. These empirical engineering models use hydrodynamic coefficient databases constructed from the forced vibration experiments on rigid cylinders. Due to the non-linearity and high-dimensionality of the problem, the current empirical VIV prediction models still have large error bounds.[25]

To solve the aforementioned problems, more advanced data analytic techniques are required. The rapid development of artificial intelligence and machine learning (AI/ML) methods in recent years offers a wealth of techniques to discover patterns in high-dimensional and non-linear data.[26–28] These characters provide a tangible solution to extract key FIV features and model their non-linearity. The recent development and application of AI/ML techniques include feature selection,[29] physics-informed neural network,[30–32] and multi-fidelity predictions.[33] Additional physical insight and improved prediction accuracy could be achieved using the synergic approach.

Given the recent progress in physics insight and modeling for flexible cylinder FIVs, this paper presents a selective review on the related topics. We first summarized the characters of structural response, hydrodynamic forces, and wake characteristics for both the isolated and multiple circular cylinders. In particular, the focus is given to the combined-IL-and-CF motion effect on flexible cylinder VIVs. Meanwhile, we discuss the interference between two circular cylinders and pay special attention to the WIVs of cylinders in a tandem arrangement. Next, we shed light on the new advancement of data-analytic techniques and their exciting applications in flexible cylinder FIV modeling. The preliminary result shows that the combination of AI/ML techniques and the physics-based model can efficiently identify key features affecting flexible cylinder FIVs. Furthermore, we can achieve a more accurate prediction of the structural response by keeping the data-driven model consistent with physical knowledge of the problem.

II. NEW PHYSICS INSIGHT INTO SLENDER BLUFF BODY VIVs

As described in the introduction, over the last decade, a number of well-controlled lab experiments, large-scale field observations and high-fidelity simulations have helped to shed light on the complex nature of the flexible cylinder FIVs. In particular, we identify the following key questions that have been well addressed in the recent research works:

(1) what is the similarity and difference of the FIV response between flexible and rigid cylinders?
(2) what is the similarity and difference between the flexible cylinder response in constant uniform flow and unsteady/non-uniform flow?
(3) what is the similarity and difference between the response of an isolated flexible cylinder FIV and multiple flexible cylinder when interfering?
(4) what is the effect of combined the IL and the CF motion on flexible cylinder structural response, fluid forces, and vortical wakes?
(5) when and how will traveling wave response dominate the flexible cylinder FIVs?
(6) what are the detailed 3D vortical wake patterns behind the vibrating flexible cylinders?
(7) what are the most influential structural and hydrodynamic features for infinitely long flexible cylinders?

A. VIV of a single flexible cylinder

1. Characters of the VIV structural response

Since Brika *et al.*[34] first conducted laboratory experiments on a flexible cylinder placed in the uniform flow, several other well controlled laboratory experiments[21,35–42] have been conducted to study the structural responses, fluid forces, and wake patterns of a flexible cylinder in the flow. Additionally, large-scale experiments in both deep water basin facilities and field[19,43–48] helped to shed some light on the response of the slender structure with a very large aspect ratio close to those used in the real ocean. Furthermore, numerical simulations including both the reduced order model, such as wake oscillator,[49–52] and high-fidelity CFD[53–58] have used to explore a large structural parameter space as well as to visualize the wake topology in detail.[21]

The uniform flexible cylinder in the uniform flow is one of the simplest models for the flexible cylinder VIVs. Despite its simple form, a rich number of phenomena have been reported, including modal transitions in both the IL and the CF directions, dual harmonics,[21] amplification of the drag forces,[19] the existence of the higher harmonic force components,[45] and variation of the top tension.[61] One of the key differences between the flexible cylinder and the rigid cylinder[62] is that the flexible cylinder can have an infinite number of structural natural frequencies and modes. Therefore, key questions may arise whether the amplitude and frequency response of the flexible cylinder may resemble those of the rigid cylinder. In addition, for the flexible cylinder, when two/multiple potential modes can be excited simultaneously, which one/ones may appear. Such questions have been demonstrated in the sketch, shown in Fig. 2.

In the experiment conducted by Huera-Huarte *et al.*,[37,38] 45% of the flexible model was in the water, creating a stepped inflow condition. Indeed, some similarities between flexible and rigid cylinders undergoing VIV were observed. When the top tension was low, the model vibrated as a tensioned beam. Three branches of initial, upper, and lower parts were observed, similar to that in the rigid cylinder response.[64] When the tension increased, the model behaved like a
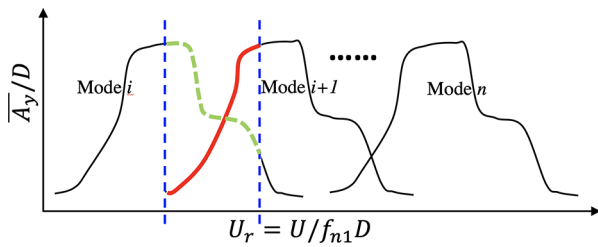
FIG. 2. Sketch of the potential amplitude response for the isolated flexible cylinder that has an infinite number of modes and natural frequencies. Questions, therefore, are raised whether its structural response may resemble that of the rigid cylinder.[59,60]

string, and the response concentrated into only the initial and upper branches.[21]

More comprehensive experiments on the long flexible cylinder over a wide range of reduced velocities were conducted by Chaplin *et al.*[35] and Fan *et al.*[21] on models of different scales at different facilities. Need to point out here, in both experiments, the effect of the tension along the flexible structure was more significant than that of the bending stiffness. Their results shared a similar trend that the model

responds with a narrow-banded single frequency, and the IL motion played an essential role in the CF vibration, as previously found in the rigid cylinder vibration.[65,66] In addition, the maximum displacement of the flexible cylinder VIV exhibited a discontinuous response pattern during the modal group switch, accompanied by the jump of the response frequency, shown in Fig. 3. Such a phenomenon has also been observed in a much larger scale experiment from the Norwegian Deep-water Program (NDP) of a 38-m-long riser model towed in the water basin.[67] Fan *et al.*[21] explained that such a frequency and displacement jump was a result of variation of the hydrodynamic coefficient distribution along the model, especially the fluid added mass.[68]

Another noteworthy larger-scale flexible cylinder experiment includes Exxon Production Research co-sponsored investigation of a tensioned steel tube, 23 m in length ($d = 4.13$ cm), exposed to uniform flow in the summer of 1981 at Castine, Maine. The results were used to construct a widely used mean drag coefficient formulation.[69,70] Depending on the current speed, the CF standing wave response was observed for the second, the third, and the fourth mode. Under rare ideal conditions, dual resonance, the CF and the IL lock-in response, was observed, which includes figure-of-eight motion and peak amplitude response of $A_y/d = 1.4$. Similar large-amplitude, figure-eight trajectories accompanied by phase-coupled IL and the CF motion were
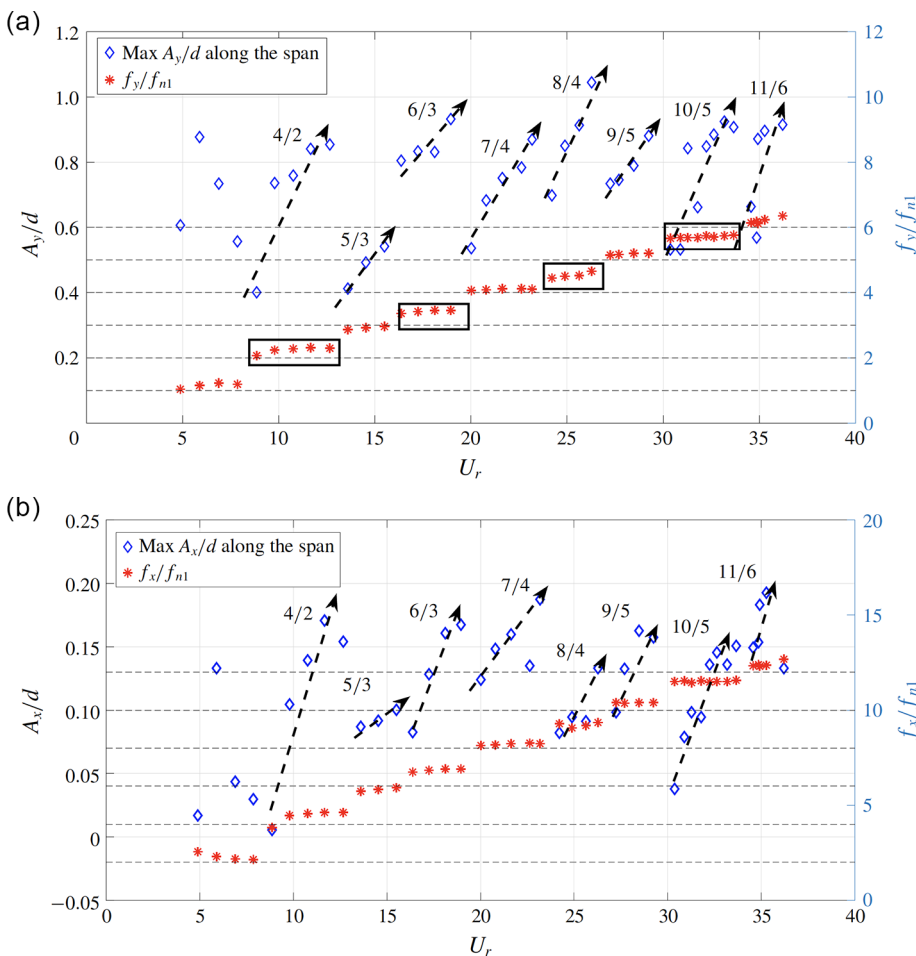
FIG. 3. Frequency ratio and maximum amplitude of the CF (a) and IL (b) displacement ($A_y/dA_x/d$) along the span vs U_r. Red stars, frequency ratio f_y/f_{n1} and f_x/f_{n1}; blue diamonds, maximum amplitude of the CF and the IL displacement. Cases in the same modal group (same dominant mode in both the IL and the CF directions) are labeled together with the black dashed arrow. Starting from $U_r = 8.84$, in the same modal group the maximum of A_y/d and A_x/d monotonically increases with U_r, but during the modal group switch, both the maximum of amplitudes and the frequency ratios jump. The CF frequency ratio f_y/f_{n1} of the "2n:n" modal group highlighted by the black box, for example modal group "6:3," shows that the actual vibration frequency is larger than the natural modal frequency predicted in still water.[21] Reproduced with permission from Fan *et al.*, Mapping the properties of the vortex-induced vibrations of flexible cylinders in uniform oncoming flow, J. Fluid Mech. **881**, 815–858 (2019). Copyright 2019 Cambridge University Press.

observed in a roughened, horizontal steel pipe exposed to a tidal flow in a Venetian estuary at Reynolds numbers (*Re*) up to 220 000.[71]

The uniform flexible cylinder in the shear flow: in real ocean conditions, the uniform current profile is seldom met, and a non-uniform flow profile[72,73] can be found everywhere. The shear flow condition may introduce fluid force of different frequencies along the flexible cylinder, and therefore, may excite multiple frequencies and multiple modes vibrations.

Vandiver *et al.*[74] first reported an experiment on a cable of 290 m in length and 4.06 mm in diameter in a vertical shear flow. Compared to the single-frequency narrow-band vibration of the flexible cylinder in the uniform flow, a very broadband response was identified. Furthermore, they found a smaller amplitude response of 0.25–0.5 diameter in the experiment than a one diameter amplitude response in the uniform flow. Similar phenomena were also observed and reported in the NDP shear flow case[44] that for the 38 m in length model in the shear flow: a strong traveling wave pattern dominated the amplitude response. Researchers suggested that the lock-in regions for the flexible cylinder in the shear flow were broader than uniform flow cases from the experiment. The possible explanation was that the effective added mass might change the natural frequency catering to the vortex shedding frequency.[75–77] These phenomena were also later observed in the Lake Seneca, and Miami I and II tests, where a larger number of sensors were installed on the flexible model.[19,78]

Using a curved sheet of wire gaze, Stansby[79] generated a shear inflow condition in the wind tunnel and studied the vortex shedding due to the CF vibration of a cylinder in the incoming flows. It was found that the vortices behind the cylinder were shed in cells, and the spanwise extent of lock-in at the cylinder frequency was affected by the inclination of shed vortices in the shear flow. Allen *et al.*[80] conducted a series of VIV tests of flexible cylinders in a circulating water channel with a test-section of 3.66 m depth. By comparing the flexible cylinder VIV response under different shear gradients, Vandiver *et al.*[13] categorized the response based on a shear parameter. They defined the shear parameter as the ratio of the change in velocity of the flow over the length of the cylinder to the spatially averaged flow velocity over the length of the cylinder. It was found that under uniform flow or highly shear conditions, some single-mode was often excited. While in mild shear conditions, single-mode dominance is rare. Frequently the response shows multiple modes and non-lock-in behavior, and there was a considerable time-domain fluctuation of modal response energy between various modes.

The Exxon Mobile[81] experimented on the flexible model of 11.48 m length and 20 mm diameter in the linearly sheared flow with a unique rotation rig. The well-controlled linearly sheared flow was imposed on the tilted flexible model. One of the key findings from this experiment was that a single frequency response near the Strouhal frequency was observed for all the cases, even for the strong shear rate ones; however, several modes coexisted even if the response appeared at a single frequency. In addition, the lock-in region of the flexible cylinder tended to locate in the high-velocity region. Therefore, the researchers concluded that the flexible cylinder VIV was classified as a single-frequency vibration in the linearly sheared flow. A similar phenomenon was observed in the simulation.[82–84]

Meanwhile, it isn't easy to generate stable and well-controlled non-linearly sheared flow in laboratory settings. Therefore, there are almost no well-documented experiments on the flexible model in the

non-linearly sheared flow. Some numerical simulations of such kinds have been performed on low *Re* cases.[85] Bourguet *et al.* simulated a flexible model in both a linearly sheared and an exponentially sheared flow, and he found that in both flows, multiple frequencies and modes would be excited.[86] However, difference[63] could be found on between the two inflow cases: in the linear shear flow, time-varying mono-frequency is excited, while in the exponentially shear flow, multiple frequencies were found to coexist at the same time and the same location, shown in Fig. 4.

The study of *the uniform flexible cylinder in the unsteady flow* is motivated by real industrial scenarios, such as an oscillatory flow that exists near the free surface in the presence of ocean waves, or offshore platform heave- or surge-induced riser motion, or the slowing varying unsteady flow caused by tides. Compared to a vast number of studies on the rigid cylinder in unsteady flow, such as cylinders in the oscillatory flow,[87–91] the number of studies on the flexible cylinder in the unsteady flow is significantly limited. Several noteworthy research studies on an oscillating flexible cylinder in the stationary flow[92–94] revealed that the response of flexible cylinder in oscillatory flow has both similarity and difference compared to that in the uniform flow. A typical response of the flexible cylinder in the oscillatory flow is shown in Fig. 5, which features an intermittent VIV response with an amplitude modulation including three phases: build-up, lock-in, and dry-out.[92]

The interesting phenomenon of the hysteresis response for the flexible cylinder[42] appeared as well in the unsteady flow, reported in several experiments.[92,95] Such response was especially prominent in the slowly varying flow cases, namely the slowing accelerating or decelerating cases.[95] A similar phenomenon was observed long before in the rigid cylinder.[96] Resvanis[95] proposed a non-dimensional unsteady flow parameter $\gamma = \frac{\partial U}{\partial t} \cdot \frac{T_n}{U_n}$ to predict whether VIV would be an issue in the time-varying flow. γ could be interpreted as the ratio of the velocity change during one cycle of the riser vibration and was found to be a good indicator of the VIV response in the time-varying flow:

(1) when $\gamma < 0.02$, the flexible cylinder response in the time-varying flow is similar to that in the steady current;
(2) when $0.02 < \gamma < 0.1$, VIV may occur, but the structural response differs from that in the steady current;
(3) when $\gamma > 0.1$, no VIV is observed for a flexible cylinder in the experiment.

Based on the new phenomena observed in the experiment of the flexible cylinder in the unsteady flow, several corresponding prediction methods have later been developed.[97–99]

Standing wave vs Traveling wave: field observations, laboratory experiments, and numerical simulations revealed that when long, tensioned cylinders were exposed to spatially non-uniform flow, they could have a standing wave response, traveling wave response, or a mixture in both the IL and the CF directions.[19,85,100,101] Traveling waves usually occur when there is a nonuniform distribution of damping (including both structural and hydrodynamic damping) along the cylinder.[102] For example, in a linearly sheared flow, the hydrodynamic damping is larger in the lower flow speed region. This leads to the elastic waves excited in the higher flow speed region to propagate and gradually decay in the lower flow speed region. Similarly, significant traveling waves generated in the bare region of a cylinder can be found to be propagating into the regions covered with fairings or strakes.[20]
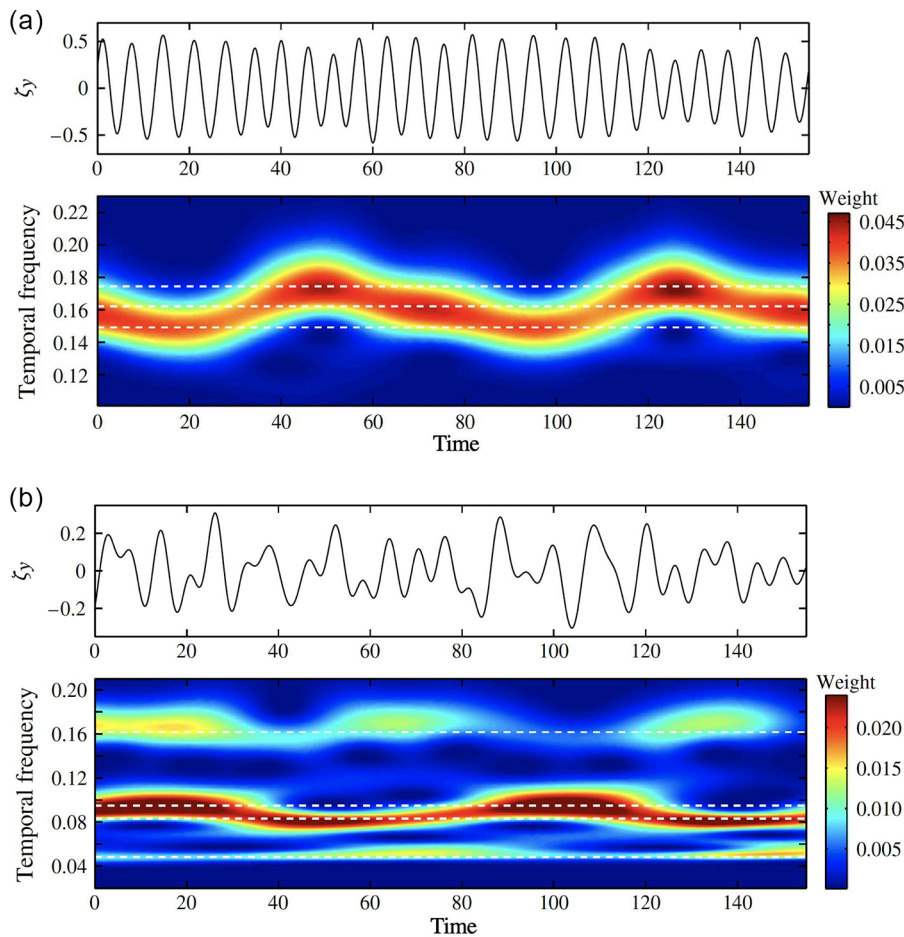
FIG. 4. Selected time series of the CF displacement and frequency content at certain location along the model as a function of time (scalogram), in the (a) narrowband (linear shear flow) and (b) broadband (exponential shear flow) response cases.[63] Reproduced with permission from Bourguet, *et al.*, "Distributed lock-in drives broadband vortex-induced vibrations of a long flexible cylinder in shear flow," J. Fluid Mech. **717**, 361–375 (2013). Copyright 2013 Cambridge University Press.

Whether the response is traveling wave-dominated or standing wave-dominated can influence the distribution of phase angles and the hydrodynamics along the cylinder. In standing wave-dominated motion, the phase angle between CF and IL motion has a 180° jump at the IL node, which is accompanied by a strong shift in the added mass coefficient.[21] In contrast, for the traveling wave-dominated VIV response, the phase angles and motion trajectories change gradually, and regions with a favorable phase angle may exist over long lengths of the pipe.[19]

To characterize the response features mentioned above, proper orthogonal decomposition (POD) was conducted to reduce the dimension of the flexible cylinder VIV from infinite degrees of freedom to a few dominant modes in the CF and the IL directions.[103,104] The mode dominance factor κ was proposed and used to characterize whether single-mode dominated the response or multiple modes were competing simultaneously. By analyzing the statistics of mode participation of flexible cylinder VIVs via moving window analysis, it was found that the IL vibration tended to be more complicated, requiring several more POD modes compared to the CF vibration. To further tell the difference between traveling waves and standing waves, a traveling wave index α was proposed. The statistics of the mode dominance factors and traveling wave indices were analyzed for the

large-scale VIV experiments. Using these parameters as inputs, the machine learning model showed that the higher harmonics of the cylinder tend to increase when the vibration would be dominated by a single mode and traveling waves.[104]

2. Hydrodynamics and wake topology of a single flexible cylinder VIVs

Rigid vs flexible, the validity of the strip theory assumption: the state-of-art prediction tools for the riser VIV are based on the validity of the strip theory,[105] which assumes that the hydrodynamic force distribution along the flexible model can be accurately captured via the hydrodynamic coefficient database constructed via rigid cylinder forced vibration with prescribed trajectories.[106–108] Such an assumption has been taken for granted for decades without much careful verification.

One of the major obstacles is that directly measuring the fluid force distribution along the flexible cylinder in the experiment is difficult. Therefore, several inverse force calculation methods were developed. Using methods of finite difference,[109] finite element,[110] least squares estimation,[111–113] and Kalman filter estimation,[111] distributed fluid forces and hydrodynamic coefficients along the flexible cylinder
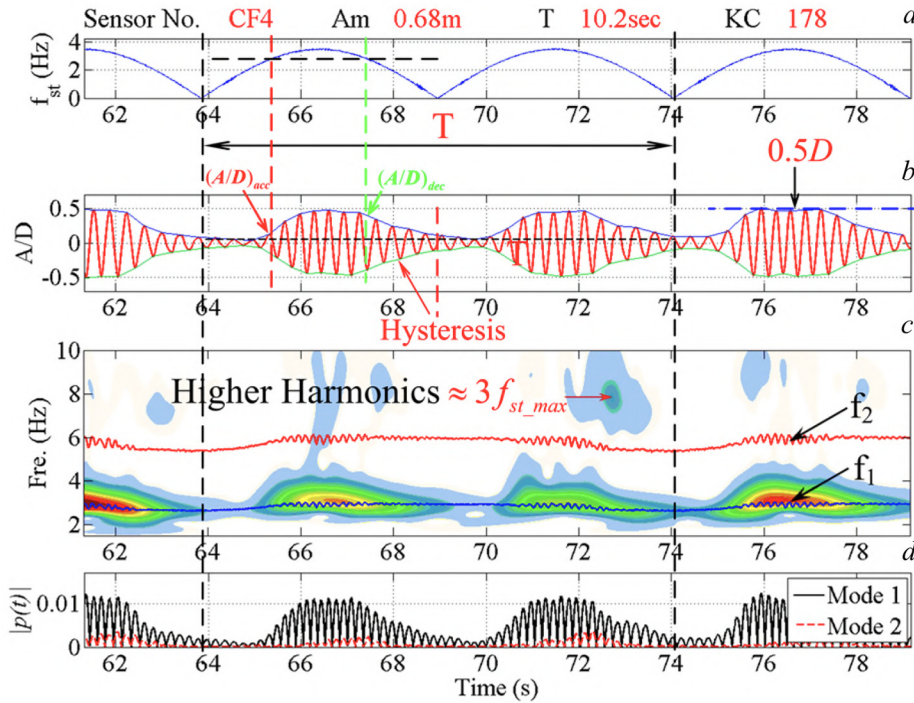
FIG. 5. A typical response of flexible cylinder in the oscillatory flow[92] at $T = 10.2s$, $KC = 178$. (a) The shedding frequency; (b) amplitude ratio; (c) response frequency; and (d) modes. Reproduced with permission from Fu et al., "Features of vortex-induced vibration in oscillatory flow," J. Offshore Mech. Arct. Eng. **136**, 011801 (2014). Copyright 2014 of American Society of Mechanical Engineers ASME.

were inversely reconstructed from the measured displacement response.[21] These inverse force calculation methods have been validated against numerical simulations and some experiments. One major limitation in these methods is that most of the techniques except the Kalman filter methods proposed by[111] are not able to quantify the uncertainty in the process or the sensor measurement. In general, the results showed that fluid force distribution along the flexible cylinder was much richer than and qualitatively different from the hydrodynamic coefficients acquired from the rigid cylinder CF-only force vibration experiment.

The development of the inverse force reconstruction methods helped to significantly enhance our understanding of the flexible cylinder fluid force distribution undergoing VIVs. For example, based on the energy conservation, Rao et al.[114] proposed a power-flow approach and successfully identified the "power-in region" a.k.a. "lock-in" region, where the positive energy transferred from the fluid to the structure along the flexible cylinder. One important finding in that study was that for bare pipes under linear shear flow, the power-in region was around 30% of the entire pipe near the high flow speed end, which was also revealed in CFD analysis.[85]

Fan et al.[21,105] used high-fidelity numerical tools, well-controlled laboratory test on flexible cylinder motion, and a robotic towing tank[115] to construct a detailed rigid cylinder hydrodynamic database.[116] They demonstrated the validity of the strip theory between the reconstructed force distribution along a uniform cylinder in the uniform flow. In addition, they predicted sectional hydrodynamic coefficients from a combined-IL-and-CF rigid cylinder hydrodynamic database. In specific, the positive C_{lv} was found in locations with a small CF amplitude and counterclockwise phase θ distribution,[117] shown in Fig. 6(c). In addition, C_{my} varied significantly along the flexible cylinder due to the effect of various θ distribution along the span,

shown in Fig. 6(d). Furthermore, span-averaged C_{mx} and C_{my} were interrelated, helping to reach a dual resonance in both the IL and the CF directions.

For VIV problems, a *vortical wake pattern* analysis is crucial for a better understanding of the mechanisms of coupled interaction between the fluid and the structure. It is rather difficult to quantitatively acquire a detailed flow visualization in the wake of the oscillating flexible cylinder from experiments. Limited work using 2D-PIV[38,118] revealed that the vortical wake patterns behind the node and anti-node sections of the flexible cylinder resembled to those observed in the rigid cylinder free vibrations.[96] On the other hand, a high-fidelity CFD result can provide an in-depth view of both cross-sectional and three-dimensional vortical wake topology,[119–125] shown in Figs. 6(e) and 6(f), respectively. Several key findings from the simulated wake behind the oscillating flexible cylinder included: (a) in the uniform flow, parallel vortex shed in spanwise cells separated by the IL nodes,[21] shown in Fig. 7, in contrast to the oblique vortex shedding pattern when the flow had an angle to the cylinder axis;[126] (b) there was a strong correlation among the sign of the cross-flow added mass, the cylinder orbit orientation and the vortex shedding mode, which is illustrated in the experiment and simulation[68] that the IL motion will strongly affect the vortex shedding pattern and the relative motion between the cylinder and shedding vortices, hence altering the fluid added mass.

3. The effect of key structural parameters on flexible cylinder VIVs

Understanding the system parameters that has a strong influence on the flexible cylinder VIVs, is key for designing, predicting, and monitoring the structural health of marine risers.
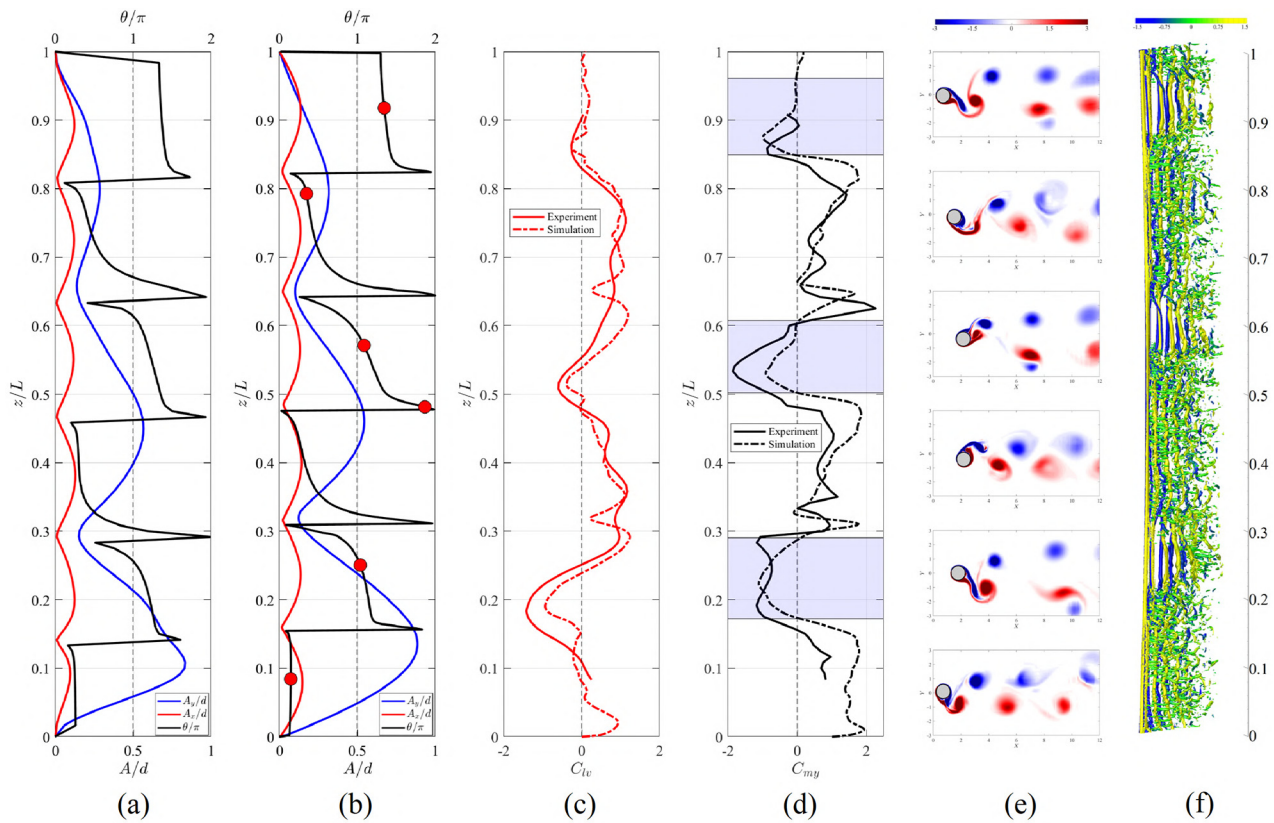
FIG. 6. Structural response and wake flow of the uniform flexible cylinder ($L/d = 240$) in the uniform current[68] at $Re = 900$. (a) *Experiment result*: blue solid line, CF displacement; red solid line, IL displacement; black solid line, phase angle between the IL and the CF trajectories (θ); black dashed line, $\theta = \pi$. (b) *Simulation result*: lines are equivalent to (a). (c) Distribution of lift coefficient in phase with velocity (C_{lv}): red solid line, experiment; red dotted line, simulation; black dashed line, $C_{lv} = 0$. (d) Distribution of added mass coefficient in the CF direction (C_{my}): black solid line, experiment; black dotted line, simulation; black dashed line, $C_{my} = 0$; the blue shade highlights the region of "P + S" vortex shedding mode. (e) *Two-dimensional* snapshots of the vorticity field at six spanwise locations highlighted by the red circles in (b): from top to bottom, $z/L = 0.9178$, $z/L = 0.7926$, $z/L = 0.5714$, $z/L = 0.4814$, $z/L = 0.2505$, and $z/L = 0.0842$. (f) A *three-dimensional* snapshot of the vortices. It is noted that the vortices are represented by iso-surfaces of $Q = 0.1$ and colored by ω_z. Reproduced with permission from Wang *et al.*, "Illuminating the complex role of the added mass during vortex induced vibration," Phys. Fluids **33**, 085120 (2021). Copyright 2021 with the of AIP Publishing.

Traditionally, the mass-damping parameter $m^*\zeta$ that was introduced by Scruton[127] has been widely used to correlate peak response amplitude for both rigid and flexible cylinders.[128] However, $m^*\zeta$ is based on structural damping only, and it does not take into account the hydrodynamic or radiation damping for flexible cylinders. By carefully following the flow of power throughout the structure under the assumption of the narrow-banded, steady-state vibration, Vandiver *et al.*[20] proposed a dimensionless damping parameter for a flexible cylinder, known as c^*. The proposed parameter can place the global structural response on a spectrum of lightly to heavily damped systems for both experimental measurements and simulation program predictions, as shown in Fig. 8. Ma[104] later demonstrated that the damping parameter c^* also plays an important role in decreasing the higher harmonics response.

Meanwhile, a wave attenuation parameter $\beta_R = c_{out}L_{out}/Z_R$ was proposed to determine when the radiation damping was dominant,[20] where c_{out} and L_{out} are the damping coefficient in the power-out region and the length of the power-out region, respectively. Z_R is the

local impedance at the boundary between "power-in" and "power-out" regions. For the tension dominated cylinder, the local impedance can be well approximated by $\sqrt{Tm}$.

It has been derived that when $\beta_R > 2.3$, the cylinder behave as if of an infinite length, where the vibration waves excited in one region propagate and die out due to structural and hydrodynamic damping before reaching the boundaries of the pipe. In this situation, the radiation damping, determined by the impedance of the cylinder Z_R, is the dominant factor for energy dissipation. Such a condition was found to happen for very long risers in shear flow[74,130,131] or risers partially covered with strakes or fairings.[20]

In 1983, a 290 m long and 4.06 mm diameter braided Kevlar cable was deployed in a shear current from a barge, moored near St. Croix in the US Virgin Islands.[74,131] It was observed that the tension-dominated cable exhibited dynamic response characteristics like that of an infinitely long system, with traveling waves leaving the excitation region and diminished to negligible levels in approximately 40 m. Even though the structural damping ratio of the pipe ζ was low, the
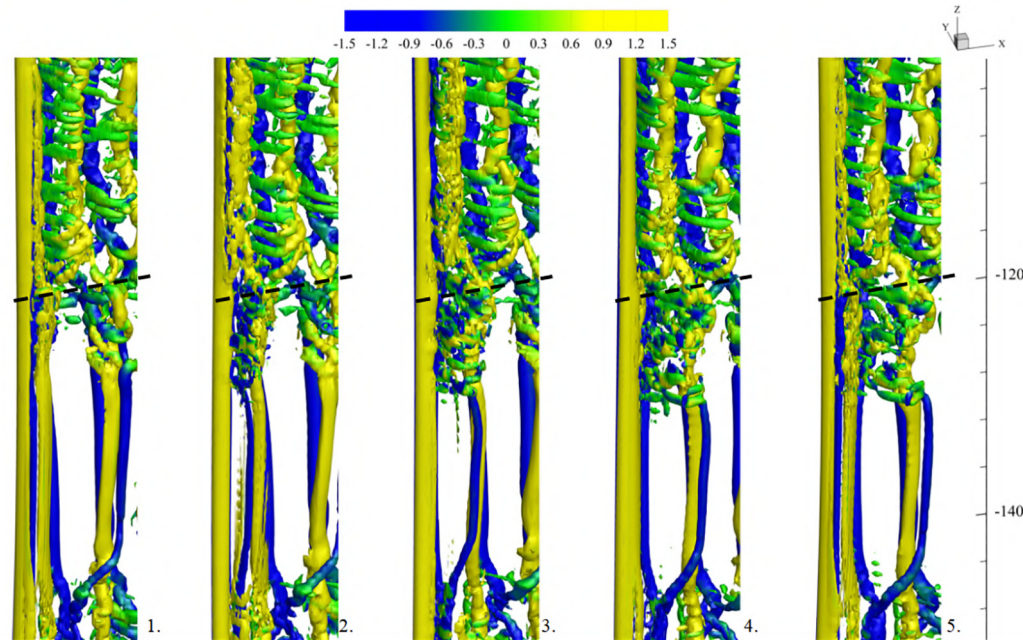
FIG. 7. A series of snapshots of the vortex shedding for flexible cylinder at $Re = 900$[21] over one period at $t = 0$, $t = \frac{1}{4}T$, $t = \frac{1}{2}T$, $t = \frac{3}{4}T$, and $t = T$ from left to right, where T is the vibration period at Ur D $U_r = 17.22$. The vortices are represented by isosurfaces of $Q = 0.1$ and colored by ω_z. Reproduced with the permission from Fan et al., "Mapping the properties of the vortex-induced vibrations of flexible cylinders in uniform oncoming flow," J. Fluid Mech. **881**, 815–858 (2019). Copyright 2019 Cambridge University Press.

observed RMS response amplitude in the power-in region was unusually small of less than half a diameter.[19] The phenomena remained a puzzle until the role of radiation damping was found to be a controlling factor in the experiment.[20]

Besides adjusting the impedance of the cylinder, the relative importance between the tension and the bending stiffness also has an effect in adjusting the natural frequency and dispersion relationship of a cylinder. To investigate how the structural mode shape could affect vortex-induced vibrations, Gedikli et al.[17] systematically altered the cylinder bending stiffness using plastic beams molded inside flexible urethane cylinders. Similar to the observations in large-scale field

FIG. 8. A^*_{rms} vs c^* for measured and predicted CF response amplitude of a 12 mm diameter pipe in 2011 Shell experiment.[20] C_{L1} and C_{L2} are two lift coefficient models in SHEAR7 program.[129]

experiments,[70] the small-scale experiments confirmed that for excitation of low mode numbers, due to symmetric drag loading, the cylinder was unlikely to vibrate with an even mode shape in the IL direction. Meanwhile, no IL mode shape changes were observed unless a CF mode shape change occurred. This observation was different from the tension-dominated model experiments.[21] In addition, Wu et al. found that the prediction of CF VIV and higher harmonics stress could be improved by taking into account the relative importance of tension with respect to the bending stiffness.[132]

Moreover, the boundary conditions are also important. Seyed-Aghazadeh et al.[133] studied the effects of symmetry breaking at the boundary of the flexible cylinder in a recirculating water tunnel. The study showed that the VIV response was very sensitive to the boundary conditions even with a small amount of asymmetry, especially in high reduced velocity regions. Similarly, Grouthier et al.[134] numerically investigated the efficiency of energy harvesting of flexible cylinders with periodically distributed dampers and with a single damper only at one end. The energy harvesting efficiency through the distributed damper was found to be sensitive to the mode of the standing-wave dominated vibration, while the efficiency of the localized damper at one end of the hanging cable was found to be driven by the traveling waves, which is more robust for energy harvesting under a range of flow speeds around the design point.
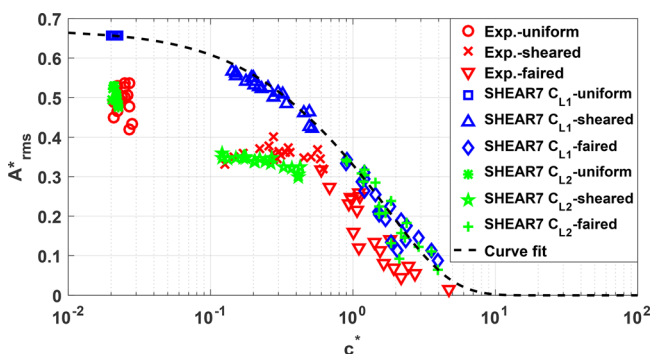
B. FIV of multiple cylinders

Due to hydrodynamic interference among the multiple cylinders,[136,137] some new concepts and phenomena arise compared to the isolated flexible cylinder VIVs. In this section, we will provide an

outline of those phenomena that are generic to the FIV of multiple flexible cylinders and pay special attention to the three aspects: (a) the characters of the structural response of multiple cylinders, (b) the hydrodynamic properties of multiple cylinders, and (c) the wake topology of flow around multiple flexible cylinders.

Since the FIV of multiple cylinders is strongly correlated with the flow interference pattern among the cylinders, we first introduce a flow interference morphology map derived from flow around two stationary cylinders, shown in Fig. 9. In the light of the classification proposed by Zdravkovich,[138] the flow interference pattern is categorized into four regimes based on wake topology: (a) proximity interference regime, (b) wake interference regime, (c) proximity-wake interference regime, and (d) no interference. For FIVs of multiple flexible cylinders, we reclassify the FIV interference regime based on the FIV structural dynamic response as follows,

(1) the proximity interference in the side-by-side arrangement;
(2) the near-wake interference in the tandem arrangement with small separation;
(3) the far-wake interference in the tandem arrangement with large separation;
(4) the proximity-wake interference in the stagger arrangement.

1. Structural response characters of multiple flexible cylinder FIVs

Huera-Huarte et al.[139,140] first conducted comprehensive experimental measurements on the FIV of two flexible cylinders in tandem arrangement over a wide range of separation gaps. Based on the different structural response pattern, they proposed the classification of the flexible cylinder FIV interference as the near-wake and far-wake interference regimes. Furthermore, they suggested that the criterion to differentiate the two wake interference regimes was whether vortex

shedding existed between the gap. In the near wake interference regime, the modal synchronization region the upstream cylinder would extend to higher reduced velocities, compared with the VIV of an isolated cylinder. However, due to the "wake shielding effect,"[141] the downstream cylinder vibration amplitude[139,142] was reduced. In contrast, in the far wake interference regime, the upstream cylinder showed the classical VIV behavior. The downstream cylinder would experience a wake-induced vibration (WIV). Considering the richer number of features of WIV, we pay special attention to the downstream cylinder response in the following content.

Compared to VIV, WIV is not well studied. The phenomenon was referred to as wake-induced galloping[143,144] or wake-induced vibration[135,145,146] in the early studies with FIV of two tandem elastically mounted rigid cylinders. The key physics insight into the rigid cylinder WIV is that the downstream cylinder can reach a much larger amplitude well beyond the synchronization region of the isolated cylinder VIV response.

Compared to the rigid cylinder WIVs, the structural response of flexible cylinder WIVs shows some different features. One of the key differences is that the flexible cylinder can have an infinite number of structural natural frequencies and modes. The first laboratory measurement of the flexible cylinder FIV response with an upstream wake interference was conducted by King and Johns.[147] Only the first modal response was excited in the experiment, and the amplitude response vs the reduced velocity was found similar to downstream rigid cylinder WIVs.

The experiment conducted by Allen et al.[149] further revealed that the increase in the upstream cylinder displacement would reduce the wake interference effect on the downstream cylinder. In contrast, the downstream would vibrate at more than one frequency. These two characters have been further investigated and confirmed in various other experimental and numerical studies.[148,150–152] The studies showed that lower modal resonance persisted over an extensive range
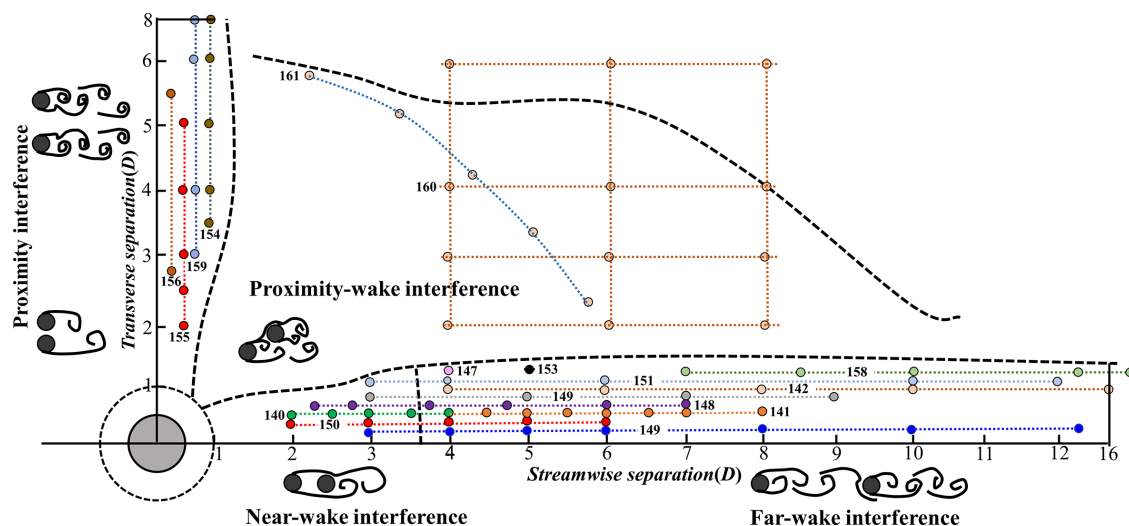
FIG. 9. The multiple flexible cylinders FIV interference regime classification and a sketch of the characteristic wake pattern for the different FIV interference regimes. A summary of the FIV structural arrangement and separation cases that have been concerned by the previous studies is included. The point at the horizontal line indicates the tandem cases, and the point at the vertical line indicates the side-by-side cases. The coordinate value of the point indicates the separation. The point of the same color indicates the separation cases from the study that is labeled by the number of it appearing in the reference list.

of reduced velocities, while the appearance of the higher modal resonance was little affected. Due to the extension of the lower modal resonance branch, the overlapping between the former modal resonance and the local modal resonance might occur, shown in Fig. 10.

When the multiple cylinders are in a side-by-side arrangement,[153] the structural FIV response is correlated with proximity interference. Particularly, the CF amplitude response of the two cylinders was found to be synchronized.[154,155] In addition, the IL amplitude response was enhanced,[156] compared to that of an isolated cylinder. While the wake interference effect can exist more than 20 diameters downstream,[157] the proximity interference effect is limited in a narrower side-by-side separation range. In specific, the proximity interference effect on the CF response is below six diameters,[154,155,158] but its impact on the IL response can reach a large value.[158]

The structural FIV response may involve both wake and proximity interference when the flexible cylinders are in a stagger arrangement. A limited number of experiments can be found, including Xu et al..[159,160] In general, understanding of the flexible cylinder FIV in a stagger arrangement is still minimal.

2. Multiple flexible cylinder FIV hydrodynamic properties and wake topology

The fluid force coefficients C_v in phase with the velocity (including C_{lv} and C_{dv}) quantify the energy transfer between fluid and structural motion. The positive C_v stands for the net energy gain from the fluid to structure, while the fluid damping effect will result in a negative C_v. The added mass coefficient can be derived from the fluid force coefficient in phase with the acceleration, and they can be used to evaluate the system's true natural frequency. The definition of these hydrodynamic coefficients remains the same between the isolated and multiple cylinders. Therefore, Lin et al.[59] first constructed a hydrodynamic database of a downstream cylinder in the wake of an upstream stationery using the CF-only forced vibration test of a rigid cylinder.

The comparison of the hydrodynamic database of a single rigid cylinder and a downstream cylinder 5 diameter behind a stationary cylinder is plotted in Fig. 11 for C_{lv} and in Fig. 12 for C_{my}. The C_{lv} contour in Fig. 11 shows that the cylinder with the upstream wake interference effect may reach a higher amplitude at a lower reduced frequency, namely, a higher reduced velocity, instead of ceasing resonance as the isolated cylinder. Such a property explains the enlargement of the resonance regime and the increase in the CF amplitude in the experiment of rigid cylinders in a tandem configuration,[135] shown in Fig. 10(a). In addition, it also helps to shed light on why the downstream flexible cylinder FIV amplitude remains a large value even in the modal resonance transition region. The C_{my} contour in Fig. 12 shows that C_{my} of the downstream cylinder decreases with the increasing reduced velocity and reaches a lower negative value than that of an isolated cylinder. The lower added mass coefficient can enlarge the synchronization region between the vortex shedding frequency and the structural FIV frequency. A limited number of works that studied the hydrodynamic coefficient distribution along the multiple flexible cylinders included the experiment[161] by Han et al. and simulation[148] by Lin et al. Their preliminary result revealed that the distributed hydrodynamic properties of a downstream flexible cylinder could still be reproduced from the hydrodynamic coefficient database measured

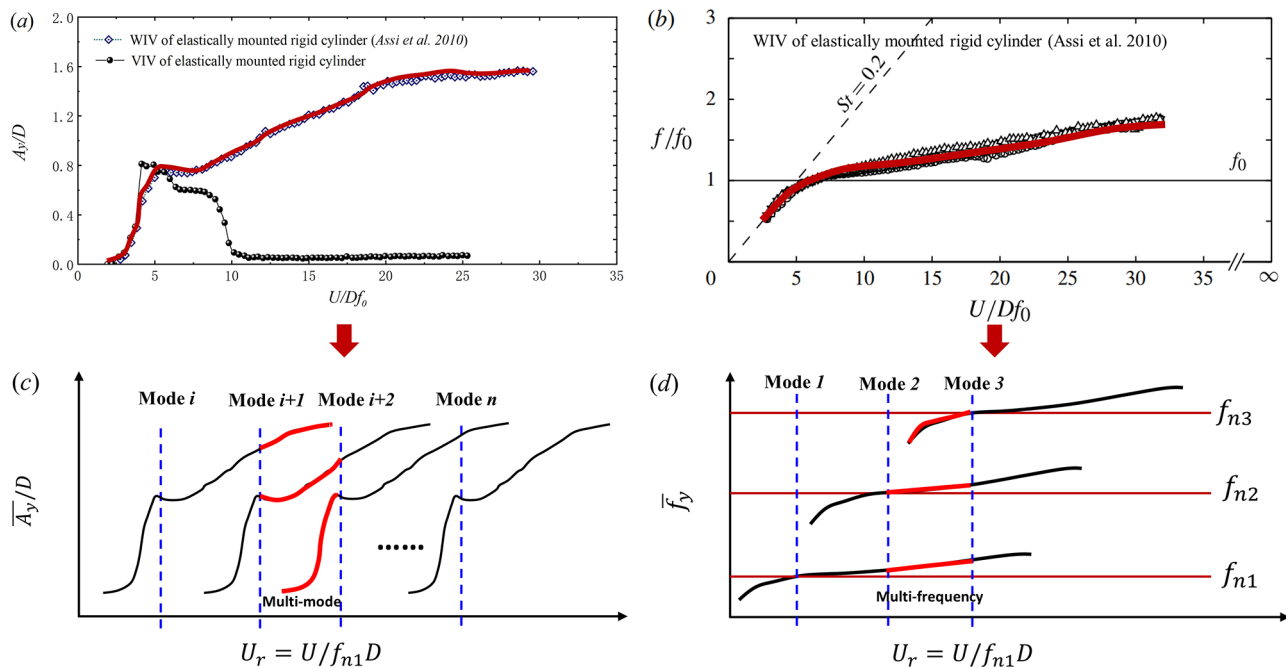**FIG. 10.** A typical WIV response of the elastically mounted rigid cylinder,[135] (a) amplitude; (b) frequency. A sketch of the potential WIV response for the slender flexible cylinder that has an infinite number of vibrational modes and natural frequencies. Due to an extension of the lower modal resonance branch, (c) multiple modes can be excited simultaneously; and (d) multiple frequencies can be excited simultaneously.
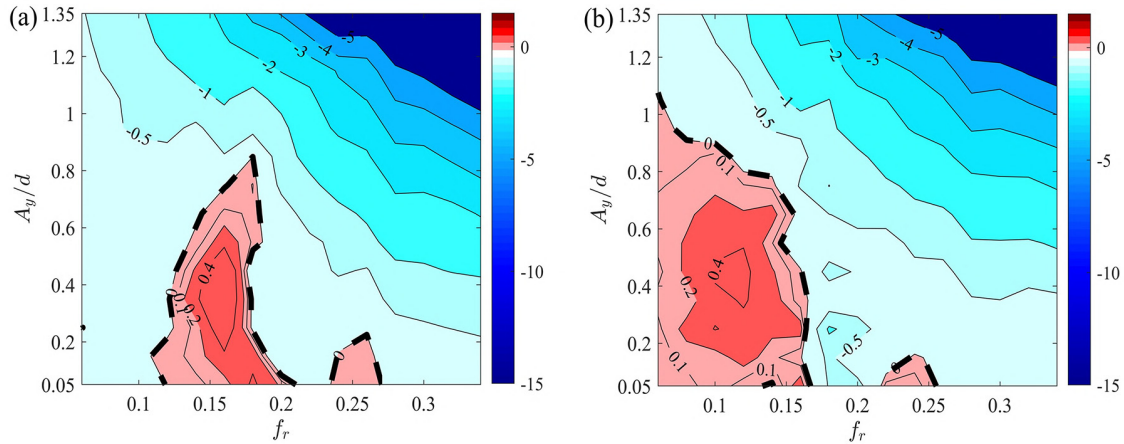
FIG. 11. Contours of excitation coefficient C_{lv} measured from the forced-vibration tests of (a) the isolated cylinder and (b) the cylinder with upstream wake interference.[59] If is found that the positive C_{lv} region of the isolated cylinder corresponds to a narrow range of f_r from 0.1 to 0.2, while the positive C_{lv} region of the cylinder with upstream wake interference is found at a lower f_r and higher A_y/d. Reproduced with permission from Lin *et al.*, "Flow-induced crossflow vibrations of long flexible cylinder with an upstream wake interference," Phys. Fluids **33**, 065104 (2021). Copyright 2021 AIP Publishing.

from the forced vibration of a rigid cylinder, shown in Figs. 13(a) and 13(b). It is noted that no hydrodynamic database for the multiple cylinders FIV with side-by-side and stagger arrangements exists.

Shown in the above section the flow visualization of the wake topology of an isolated cylinder is an essential tool to understand the underlying FSI mechanism of the flexible cylinder VIV. Similarly, such studies are key to reveal the fundamental fluid process of the multiple flexible cylinder WIVs. King and John[147] were the first to measure the wake pattern of the flexible cylinders FIV with wake interference in the experiment. Together with later works by Brika *et al.*[157] and Huera-Huarte *et al.*,[139] the studies revealed that the tandem flexible cylinder structural response and vortical wake pattern were highly correlated with the gap distance between the two cylinders. Due to the

technique limitation, the above experimental flow measurements were primarily focused on the wake pattern on a certain cross-sectional of the model and neglected the 3D wake effect.

Numerical simulation is an alternative and complementary approach to reveal 3D wake topology along the model span. In the past numerical studies,[148,162,163] one of the key findings obtained is that the correlation length of the spanwise wake vortical structure can be not only modified by the structural motion but also by the wake interference effect from the other cylinder.[162] Lin *et al.*[148] first revealed that the wake interference process is distributed along the flexible model span. The wake interference effect is highly associated with the coherence of upstream wake vortices. As shown in Fig. 13, when the vortex from upstream wake is torn apart by the downstream cylinder
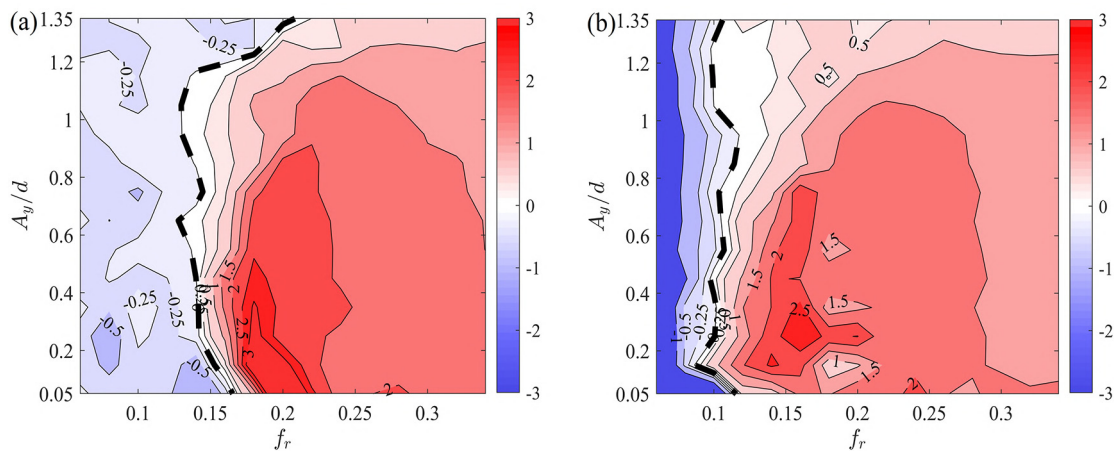
FIG. 12. Contours of added mass coefficient C_{my} measured from the forced-vibration tests of (a) the isolated cylinder and (b) the cylinder with upstream wake interference.[59] It is found that the minimum C_{my} of the isolated cylinder is larger than that of the cylinder with the upstream wake interference reaches. Meanwhile, contour line of $C_{my} = 0$ for the cylinder with the upstream wake interference is found at a smaller f_n compared to that of the isolated cylinder. Reproduced with permission from Lin *et al.*, "Flow-induced crossflow vibrations of long flexible cylinder with an upstream wake interference," Phys. Fluids **33**, 065104 (2021). Copyright 2021 AIP Publishing.
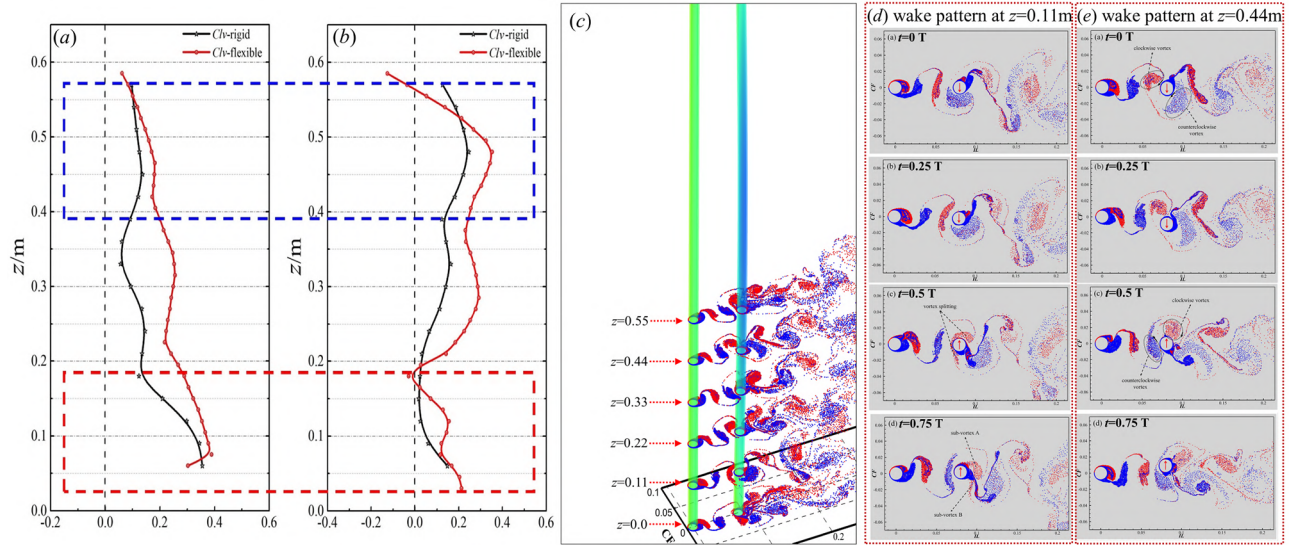
FIG. 13. Case $U_r = 7.3$:[148] The distribution of the lift coefficients in phase with the velocity C_{lv} along the isolated flexible cylinder (a) and the flexible cylinder with upstream wake interference (b) (the red value is reconstructed from the forced vibration test of the rigid cylinder; the black value is calculated from the FIV simulation of the flexible cylinder). (c) Instantaneous wake vortex pattern along the flexible cylinder span for the VIV of isolated cylinder. (d) Instantaneous wake vortex pattern over one period of cross-flow oscillation at two representative span-wise locations $z = 0.11$ m and $z = 0.44$ m for the FIV with upstream wake interference at (a) $t = 0$, (b) $t = 0.25T$, (c) $t = 0.5T$, and (d) $t = 0.75T$. Reproduced with permission from Lin et al., "Flow-induced crossflow vibrations of long flexible cylinder with an upstream wake interference," Phys. Fluids **33**, 065104 (2021). Copyright 2021 AIP Publishing.

[Fig. 13(d)], the hydrodynamic coefficient of the downstream cylinder shows higher similarity with the isolated cylinder [Figs. 13(a) and 13(b)]. For the limitation of numerical study with multiple flexible cylinder FIV, the physics insight of 3D wake topology still needs to be more addressed in the future.

C. Section summary

The new development of technologies in laboratory testing, numerical simulations, and field monitoring has significantly enhanced our understanding of the complex nature of the flexible cylinder FIVs. The significant improvements focus on the relationship between flexible and rigid cylinder FIV responses, the effect of combined the IL and the CF motions, flexible cylinder response in unsteady and non-uniform inflow conditions, especially the wake and proximity interference of multiple flexible cylinders, and most influential structural and hydrodynamic features for FIVs of the flexible cylinder with large aspect ratios. The new progress not only provides us an insightful and solid foundation for more accurate, flexible cylinder FIV modeling but also opens many more interesting questions, including but not limited to, as follows,

(1) how may we build and apply systemic rigid cylinder hydrodynamic databases (large parametric space) to predict FIVs of the flexible cylinder with complex configurations and in complex environments?

(2) how can we extend our laboratory and numerical study to more realistic conditions for flexible cylinder FIVs, such as a large Reynolds number ($\sim O(10^5)$), large aspect ratios [$\sim O(10^4)$], and turbulent non-uniform inflow?

(3) if there is one, what is the unified relationship of FIVs of multiple cylinders (cylinder arrays), and how may we build prediction methods for them?

(4) how may we better interpret laboratory studies to better monitor and manage structural integrity of the flexible structures FIVs in their lifetime?

III. AI/ML TECHNIQUES FOR MODELING FLEXIBLE BLUFF BODY FIVs

As described in the above sections, improving the data acquisition and analysis methods has driven new physics insight into and proposed new modeling of the flexible cylinder FIVs. However, as listed in the questions for future research, the complexity of the problems increases exponentially with more extensive input variables. A brute-force parametric search is laborious or even virtually impossible using classical research tools, given the problem's high dimensionality.

In recent decades, the world has witnessed explosive progress in Artificial Intelligence and Machine learning (AI/ML), especially the deep learning methods. Successful demonstrations can be found in various tasks, including image recognition,[164] natural language processing,[165] gaming,[166] and life science.[28] In particular, AI/ML offers a wealth of techniques to discover patterns in high-dimensional data. Therefore, it provides a tangible solution to understand and model the complex nonlinear dynamics commonly encountered in the FSI problems.[167–169] In the last five years, we have observed that the FSI research community[170–173] started to enthusiastically embrace the rich venue of the powerful AI/ML tools to address various fluid and structural coupling problems at a greater scale and a broader scope.

This section reviews several preliminary implementations of AI/ML tools in understanding and modeling the complex behavior

of flexible cylinder FIVs. We foresee both exciting opportunities and new challenges in the future.

A. AI-Enhanced feature identification and extraction

Extremely long flexible cylinder FIVs in deep water involve many physical variables, such as Strouhal number St, Reynolds number Re, mass ratio m^*, structural damping parameter c_s, aspect ratio L/d, top tension, and model configurations. It is essential to identify the most critical parameters for robust VIV response prediction among all the variables. With the development of AI/ML, data-driven models are becoming increasingly important to uncover the underlying physics from spatial-temporal data. For example, Rudy et al.[174] developed a sparse regression method, which can discover several governing partial differential equations of a system from measured time series in the spatial domain. Based on a variant of the sparse identification of non-linear algorithm, Li et al.[175] built a data-driven, time-dependent model to explain the nonlinear, time-varying aero-elastic interaction between a suspension bridge and wind. Distinct regimes of self-excited effects are found for different clusters of the data-driven models.

Ma et al. used a fully connected deep neural network model and a sparsity-promoting technique[176] to develop a sequential feature selection method for flexible cylinder FIV feature identification.[103,177] For example, they chose the CF amplitude response as the prediction target. They found that the predictions using the three already known essential parameters, including Re, c^*, and the shear parameter, were not accurate enough. They revealed that the coupling between the IL and the CF vibration could significantly improve the prediction. However, interpretation of these neural network models showed that the relationship identified in the models might not be consistent without the prior physical knowledge from decades of experimental observations.

To resolve the problem mentioned above, an improved neural network model that could satisfy the prior physical trend was proposed.[178] An error metric was added in addition to the prediction error to reveal whether the input features satisfy the imposed prior physical trend constraints or not. Even though several features such as mode number and Re were highly correlated, the ML model with prior constraints could distinguish their effects. The model suggested that the response amplitude increased with Re at the same vibration mode

but decreased as the vibration mode shifted to the next higher value. In linear shear current, the response amplitude tends to be more prominent when the response is single-mode dominated.[104]

Another example to identify the key VIV feature is demonstrated by Wu et al.[132] to improve the semi-empirical prediction models for flexible cylinder VIV. They introduced a new method to apply adaptive hydrodynamic parameters for different riser responses classification. The response data from various experiments were grouped into different sets/categories by data clustering algorithms. Each group was linked with several parameters, including the mode number, the dominance of traveling vs standing waves, the importance of bending stiffness, and the significance of third-order harmonic stress. Based on the classified groups, different hydrodynamic databases were then selected in the semi-empirical prediction. Similarly, Riemer-Sorensen et al.[179] used density-based clustering to investigate the relations between the features of the current profile and the statistical properties of the flexible cylinder vibrations in three-dimensional current. A random forest model was used to predict the vibration amplitude based on the local current conditions and position on the riser, whose prediction outperformed the empirical VIV prediction tools designed based on two-dimensional flow conditions.

In the field, risers will face various problems over time, such as bio-fouling,[180] structural damage,[181] and aging[182] that inevitably change the structural properties significantly. Such changes result in long-time structural monitoring, a challenging task[183] that requires not only an identification of the critical structural features but an accurate online structural property estimation and damage monitoring.[184–187]

A robust mathematical framework is constructed to address the aforementioned issue by estimating structural parameters of flexible cylinder undergoing VIVs in a sense to predict the life span of the structure through the changes in the parameters.[188] Shown in Fig. 14, this framework is accomplished by applying *physics-informed neural networks* (PINNs).[31] The PINN is a physics-informed deep learning algorithm to solve the forward and inverse problems involving partial differential equations by employing a deep neural network to approximate the unknown function. The PINN and its different variations have been successfully employed in many physical problems, such as discovering turbulence models from scattered/noisy measurements,[32]
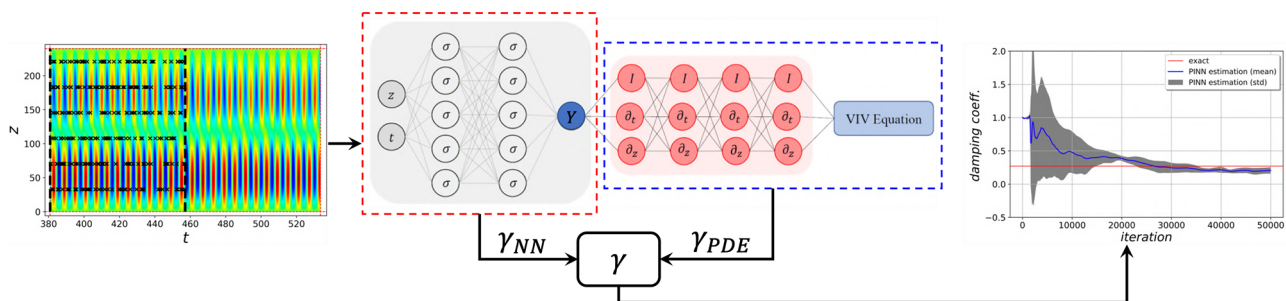
FIG. 14. The schematic of using a plain fully connected neural network structure of PINNs to learn flexible cylinder unknown structural damping. The gray shaded part highlighted by the red line dashed line is the neural network parameterized by σ, where the input layer takes the two coordinates z and t from the simulation data, and the output layer is the η_{NN}. The red shaded part highlighted by the blue line dashed line constructs the VIV equation residual with model parameters q. The loss function is composed of both terms coming from the network and the equation residual and is used to learn the unknown structural damping. Reproduced with permission from Kharazmi, et al., "Inferring vortex induced vibrations of flexible cylinders using physics-informed neural networks," J. Fluids Struct. **107**, 103367 (2021). Copyright 2021 Elsevier Science & Technology Journals.

high speed flows,[189] and stochastic differential equation by generative adversarial networks.[190,191] In detail, Kharazmi et al.[188] model the flexible cylinder as a linear tensioned beam equation coupled with nonlinear hydrodynamic forces from fluid flow. The data used to train the model were obtained from direct numerical simulations.[105] The PINN approach was found to be robust in training the data from simulations. The approach is promising to be integrated into a real-time structural health monitoring framework, where the data are obtained from field measurements/experimental observations, and the changes in the health condition of structures could be monitored.

B. Construction of the optimal FIV hydrodynamic database

In the last several decades, various numerical models have been proposed to model and predict the flexible cylinder FIVs. A comprehensive review of some reduced order empirical models and fully coupled CFD simulations for VIV prediction can be found in the study by Gabbai et al.[5]

High-fidelity CFD tools, such as large eddy simulation (LES) and direct numerical simulation (DNS) that couples the fluid motion and structural vibrations, have shown great promise to shed light, especially on the vortical wake topology.[21] However, due to the enormous resources required for CFD simulations, empirical models have been and still are the main tools for efficient offshore structure's VIV design, prediction, and monitoring. Some widely used codes include VIVANA,[24] VIVA,[23] and SHEAR7.[22] In these models, the fluid force on the slender structures is modeled as a nonlinear function of structural vibration amplitude, frequency, and the current profile. Such fluid forces are often measured in the laboratory via rigid cylinder forced vibration experiments and summarized as the hydrodynamic coefficient database. The first such database widely used was compiled by Gopalkrishnan[192] for the CF-only rigid cylinder vibration. These empirical methods capture some VIV key characteristics, such as the lock-in phenomenon.

However, these empirical models involve assumptions of empirical coefficients without a well-defined range of applications. Whether the models are valid in more complicated fluid environments, such as that with a higher Reynolds number and IL motions' effect, is still under research. Besides, these empirical prediction programs that assume the validity of the strip theory rely heavily on the accuracy of hydrodynamic databases obtained from forced vibration experiments to model the sectional forces distributed along the flexible cylinder length.

A new robotic intelligent towing tank was established by Fan et al.[116] and helps to explore the hydrodynamic coefficient affected by a large number of parameters by automatically conducting adaptive experiments. However, this new tool is still not adequate to construct a complete hydrodynamic database, as various studies have shown that these coefficients are sensitive to several parameters, including Reynolds number,[193] riser configuration,[59] turbulence in the oncoming stream, and surface roughness.[194] Hence, systematic development of a hydrodynamic database is virtually impossible due to large input parametric space. Furthermore, long-term effects such as equipment aging and bio-fouling inevitably alter the hydrodynamic coefficients throughout the lifetime of a riser, making prediction and monitoring even more challenging.

To address the problem mentioned above, Rudy et al.[195] propose a new methodology for determining parametric forms of hydrodynamic databases that can be trained with sparse sensors along the length of a riser, shown in Fig. 15. The critical element of such a proposed methodology lies in the inference of a parametric hydrodynamic database representation. The structure of the proposed databases is informed by experiments performed on rigid cylinders using both free and forced vibrations and tested on large-scale experiments using flexible cylinders. They show that the proposed method can yield more accurate predictions for VIV amplitude and frequency both in the case of rigid and flexible cylinder experiments, demonstrated by the sample case from the Norwegian deepwater program (NDP) test in Fig. 16.

C. Data assimilation using multi-fidelity modeling

As discussed in Sec. III B, systematic development of a single hydrodynamic database is virtually impossible. Therefore, Meng et al. developed the "VIV-MFnet,"[196] a multi-fidelity fast vibration inference system by integrating low fidelity, low cost, semi-empirical prediction tools with high fidelity, high cost numerical, and experimental approaches.

The key idea of multi-fidelity modeling was to discover the cross correlation between the low- and high-fidelity data rather than approximating the high-fidelity data directly. Combining a dense set of data from a low fidelity model because of its low cost of use, with a relatively sparse set of experimental and field measurements that are
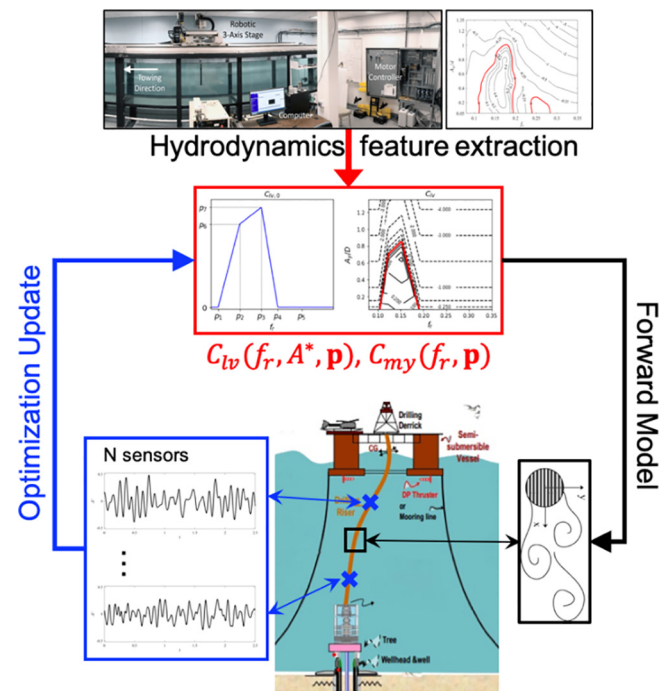
FIG. 15. Predictions of the marine riser dynamics, using optimally learned hydrodynamic databases. First, parametric models of the hydrodynamic coefficients of bluff body VIV are derived from rigid cylinder forced- and free-vibration experiments. Based on the forward model that models the physics of the problem and real-time measurements from a few sensors located along the riser, the parameters are updated via optimization to construct an optimal hydrodynamic database and hence provide an improved structural response prediction.

FIG. 16. Evolution of VIVA prediction on the NDP experiment no. 2182 (uniform velocity $U = 2.0\,\text{m/s}$) at iteration 0 (first row), iteration 2 (second row), iteration 4 (third row), and iteration 6 (fourth row). In the left column, the solid black line shows the experimental result; the red dashed line shows the nominal VIVA prediction, and the blue dashed line shows the VIVA prediction with corresponding learned hydrodynamic databases that are shown in the right column for C_{lv}. Additionally, the measured frequency re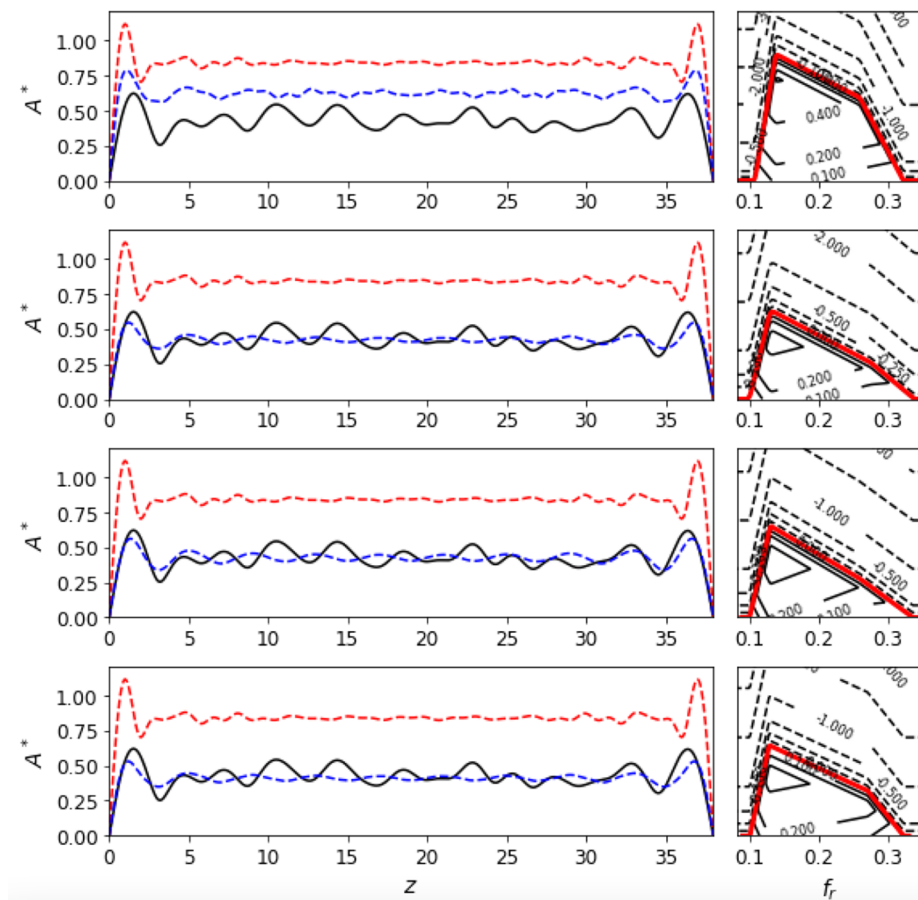sponse is 10.23 Hz in the experiment, the nominal VIVA prediction is 12.54 Hz, and with the improved hydrodynamic database, the predicted frequency response evolves as 10.71 Hz (iteration 0), 10.62 (iteration 2), 10.56 (iteration 4), and 10.63 (iteration 6). Reproduced with permission from Rudy *et al.*, "Learning optimal parametric hydrodynamic database for vortex-induced crossflow vibration prediction of both freely-mounted rigid and flexible cylinders," in *The 31st International Society of Ocean and Polar Engineering Conference* (OnePetro, 2021). Copyright 2021 International Society of Ocean and Polar Engineering.

expensive to obtain, a faster and more accurate prediction result can be obtained. Such a methodology has been implemented in various applications, such as optimal hydrofoil design,[198] polymer bandgap prediction,[199] steady flow estimation,[200] composite structures construction,[201] and modeling the biological response of growing tissues.[202]

Conventional multi-fidelity modeling approaches work well for cases in which the correlation is easier to obtain than the high-fidelity function itself, using Gaussian process regression (GPR)[203–205] or deep neural networks.[206,207] However, the correlation between the low- and the high-fidelity data for the flexible cylinder FIV prediction is much more complicated than the high-fidelity function due to phase errors between the multi-fidelity data. In addition, increasing input dimensions of flexible cylinder FIV spatial response will lead to higher computational costs. To address these issues, Meng *et al.*[196] developed a new algorithm to in the modal space and resolve the complicated correlation caused by the phase error between the low- and high-fidelity data by adding more dimensions, i.e., shifts of low-fidelity functions, to the input space. Such a methodology and a demonstration of sample results are shown in Fig. 17.

D. Section summary

In recent years, the leap of artificial intelligence and machine learning techniques has brought revolutions in different research areas, from the traditional investigation to data-driven modeling. Inevitably, a complex FSI problem such as flexible cylinder FIVs can benefit from AI/ML tools capable of discovering and modeling complex patterns in high-dimensional data. This section reviewed several successful but preliminary implementations of AI/ML tools in understanding and modeling flexible cylinder FIVs, including feature extraction and inference using clustering and PINNs, optimal hydrodynamic database construction via active learning, and multi-fidelity data fusion.

The aforementioned AI/ML developments for flexible cylinder FIVs are still in their preliminary stage. However, they draw a future with a completely different procedure of a data-driven and physics-informed assessment FIV models, a digital twin of a marine riser ("DigiMaR"),[197] shown in Fig. 18. In specific, ideally, a well-designed and trained DigiMaR system will utilize various sources of training data, including real-time field sensor data, well-controlled laboratory experimental data, CFD simulations, extracted databases, semi-empirical codes, and existing knowledge of the underlying physical models. As a result, the DigiMaR system can efficiently use the streaming data from a few field sensors to accurately reconstruct the motion of marine risers and provide fatigue damage prediction.

Cautiously, we would also like to point out that though AI/ML techniques have the potential to address various FSI problems at a
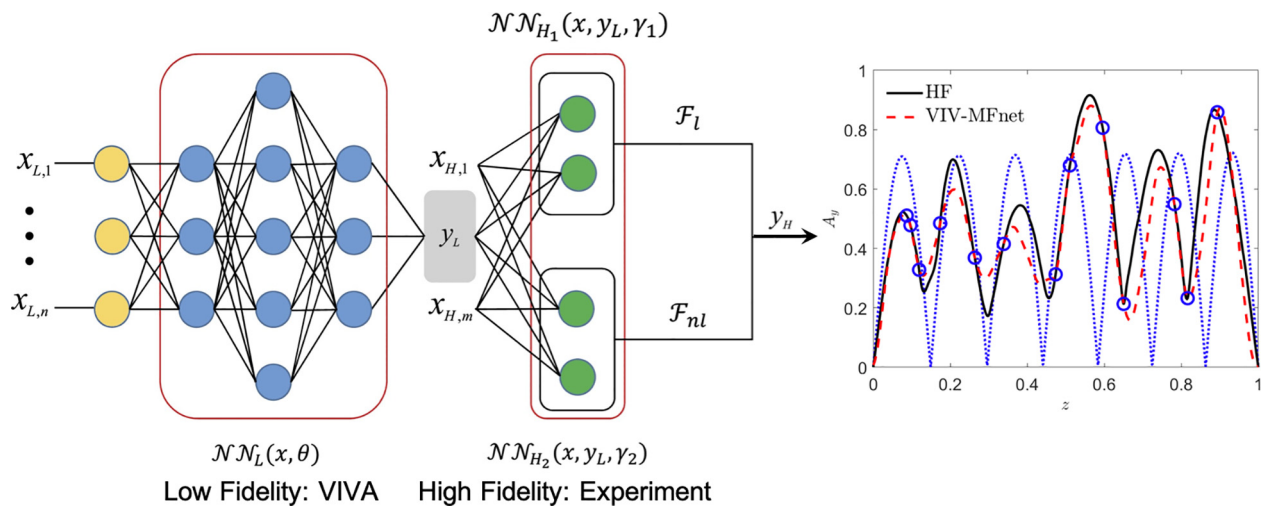
FIG. 17. Multi-fidelity predictions of displacements for uniform flow past a flexible cylinder at $U_r = 35.28$. Left panel: low- and high-fidelity data. LF: low-fidelity data from the VIVA model, HF: high-fidelity data from the experiments.[21] Right panel: correlation between the low- and high-fidelity data. Right panel: the blue dotted line: low-fidelity training data; the blue circle: high-fidelity training data; the black solid line: the experimental data; the red dashed line: the learned result. Reproduced with permission from Meng *et al.*, "A fast multi-fidelity method with uncertainty quantification for complex data correlations: Application to vortex-induced vibrations of marine risers," Comput. Methods Appl. Mech. Eng. **386**, 114212 (2021). Copyright 2021 Elsevier Science & Technology Journals.
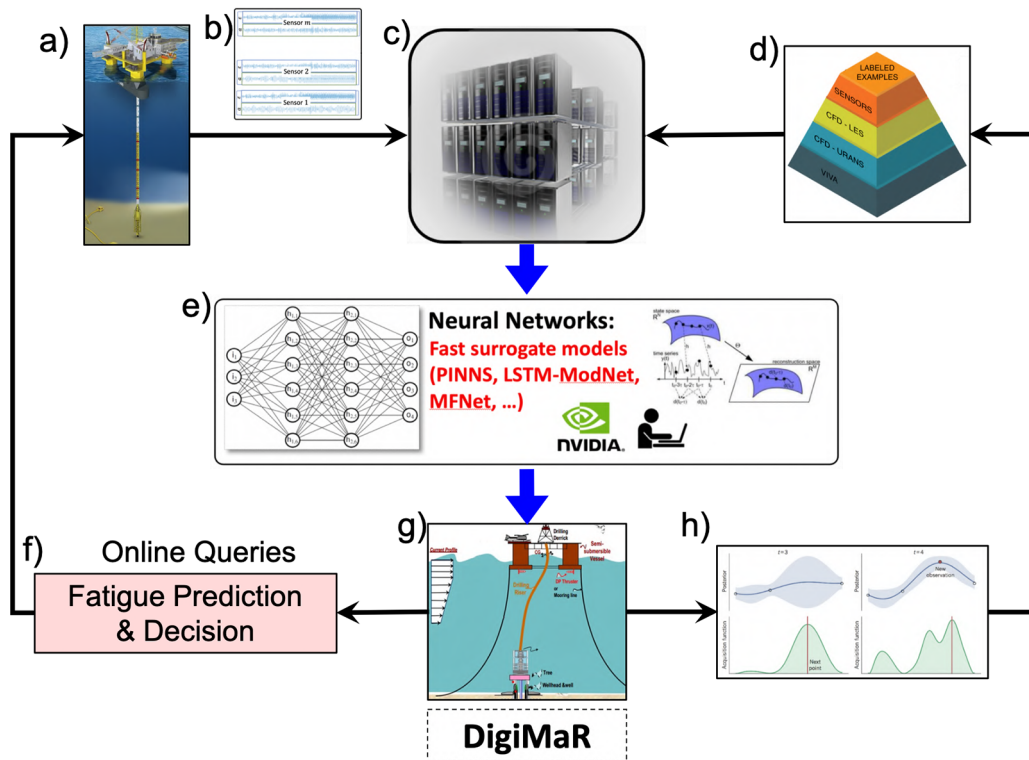
FIG. 18. DiGiMaR: a digital twin of marine risers. DiGiMaR is A data-driven assessment model based on several sources of multi-fidelity data, underlying physical model, and streaming field sensor measurements.[197] The major components include (a) marine riser system; (b)streaming data from sparse sensors; (c) data cluster; (d) several sources of multi-fidelity data; (e) data-driven reduced order model; (g) physics model; (f) structural monitoring and management tools; and (h) active learning algorithm.

greater scale and a broader scope, these data-driven and ML-assisted fluid analysis methods are still in their infancy. Therefore, caution is required to select and apply appropriate ML techniques on fluid analysis to avoid overly optimistic and simplified technology transfer, as blind prediction without any prior knowledge of the flow physics may lead to unrealistic solutions.[208]

IV. CONCLUSION

In this paper, we conducted a selective review of the progress in physics insight and modeling of flexible cylinder flow-induced vibrations over the recent decades. First, we summarized the characters of structural response, hydrodynamics, and the impact of structural properties for both the isolated circular cylinders and multiple circular cylinders. The recent advancement in wake topology analysis of flexible cylinder VIV improves the understanding of the mechanisms of coupled interaction between the fluid and the structure, such as the strong correlation among the sign of added mass, the cylinder orbit, and the vortex shedding mode from the flexible cylinder in the uniform flow and the distinct hydrodynamic interference feature. Second, we summarized the improvement of flexible cylinder FIV modeling with advanced AI/ML techniques. Feature selection and extraction techniques were found to help identify critical features of flexible cylinder FIV. The combination of AI/ML techniques and physics-based models is more robust in solving inference problems. Furthermore, the AI/ML techniques help optimize the database of hydrodynamic coefficients, and the multi-fidelity approach is found to improve the response prediction accuracy and quantify the prediction uncertainty. The framework of using AI techniques to construct a digital twin for marine risers was also presented.

AUTHOR DECLARATIONS
Conflict of Interest

The authors have no conflicts to disclose.

Author Contributions

L.M. and K.L. are first authors and contributed equally. D.F. acquired the funding. All authors provided critical feedback and helped shape the research, analysis, and manuscript.

DATA AVAILABILITY

The data that support the findings of this study are available within the article

NOMENCLATURE
Symbol and name

Symbol	Name
A_y	CF amplitude
A_x	IL amplitude
$c_s = 2m\omega\zeta$	structural damping coefficient
$C_{lv} = \frac{2F_y^0}{\rho U^2 DL}\sin(\phi_y)$	lift coefficient in phase with velocity
$C_{dv} = \frac{2F_x^0}{\rho U^2 DL}\sin(\phi_x)$	drag coefficient in phase with velocity
$C_{my} = \frac{4m_{ay}}{\rho\pi D^2 L}$	added mass coefficient in the CF direction
$C_{mx} = \frac{4m_{ax}}{\rho\pi D^2 L}$	added mass coefficient in the IL direction
$\overline{C_d} = \frac{2\overline{F_x}}{\rho U^2 DL}$	mean drag coefficient
$c^* = \frac{2c\omega}{\rho U_{rms}^2}$	dimensionless equivalent damping
d	Cylinder diameter
EI	bending stiffness
$f = \frac{\omega}{2\pi}$	response frequency
f_{nm}	mth natural frequency
L	Model length
L/d	aspect ratio
$m^* = \frac{4m}{\rho\pi D^2 L}$	mass ratio
n_{cf}	CF mode number
n_{il}	IL mode number
$Re = \frac{Ud}{\nu}$	Reynolds number
T	tension
U	flow speed
$U_r = \frac{U}{f_{n1}d}$	reduced velocity
$V_r = \frac{U}{fd}$	true reduced velocity
$Z_R \approx \sqrt{Tm}$	impedance of a tensioned cable
μ	mass per unit length
ρ	fluid density
ν	fluid kinematic viscosity
ζ	structural damping ratio
θ	phase between the CF and the IL motion
ϕ	phase between force and motion
ϕ_x	phase between the drag and the IL motion
ϕ_y	phase between the lift and the CF motion

REFERENCES

[1]T. Sarpkaya, "Vortex-induced oscillations: A selective review," J. Appl. Mech. **46**, 241–258 (1979).

[2]P. W. Bearman, "Vortex shedding from oscillating bluff bodies," Annu. Rev. Fluid Mech. **16**, 195–222 (1984).

[3]T. Sarpkaya, "A critical review of the intrinsic nature of vortex-induced vibrations," J. Fluids Struct. **19**, 389–447 (2004).

[4]C. H. K. Williamson and R. Govardhan, "Vortex-induced vibrations," Annu. Rev. Fluid Mech. **36**, 413–455 (2004).

[5]R. D. Gabbai and H. Benaroya, "An overview of modeling and experiments of vortex-induced vibration of circular cylinders," J. Sound Vib. **282**, 575–616 (2005).

[6]C. H. K. Williamson and R. Govardhan, "A brief review of recent results in vortex-induced vibrations," J. Wind Eng. Ind. Aerodyn. **96**, 713–735 (2008).

[7]R. A. Kumar, C. Sohn, and B. H. L. Gowda, "Passive control of vortex-induced vibrations: An overview," Recent Pat. Mech. Eng. **1**, 1–11 (2008).

[8]X. Huang, H. Zhang, and X. Wang, "An overview on the study of vortex-induced vibration of marine riser," Int. J. Mar. Sci. **27**, 95–101 (2009); available at https://en.cnki.com.cn/Article_en/CJFDTotal-DHHY200904014.htm.

[9]P. W. Bearman, "Circular cylinder wakes and vortex-induced vibrations," J. Fluids Struct. **27**, 648–658 (2011).

[10]X. Wu, F. Ge, and Y. Hong, "A review of recent studies on vortex-induced vibrations of long slender cylinders," J. Fluids Struct. **28**, 292–308 (2012).

[11]J. Wang, D. Fan, and K. Lin, "A review on flow-induced vibration of offshore circular cylinders," J. Hydrodyn. **32**, 415–440 (2020).

[12]J. M. Dahl, "Vortex-induced vibration of a circular cylinder with combined in-line and cross-flow motion," Ph.D. thesis (Massachusetts Institute of Technology, 2008).

[13]J. K. Vandiver, D. Allen, and L. Li, "The occurrence of lock-in under highly sheared conditions," J. Fluids Struct. **10**, 555–561 (1996).

[14]W. Chen, Q. Zhang, H. Li, and H. Hu, "An experimental investigation on vortex induced vibration of a flexible inclined cable under a shear flow," J. Fluids Struct. **54**, 297–311 (2015).

[15]C. Ji, Y. Hua, D. Xu, G. Xing, and W. Chen, "Numerical simulation of vortex-induced vibration of a flexible cylinder exposed to shear flow at different shear rates," Chin. J. Theor. Appl. Mech. **50**, 21 (2018).

[16]J. Wu, H. Lie, C. M. Larsen, S. Liapis, and R. Baarholm, "Vortex-induced vibration of a flexible cylinder: Interaction of the in-line and cross-flow responses," J. Fluids Struct. **63**, 238–258 (2016).

[17]E. D. Gedikli, D. Chelidze, and J. M. Dahl, "Observed mode shape effects on the vortex-induced vibration of bending dominated flexible cylinders simply supported at both ends," J. Fluids Struct. **81**, 399–417 (2018).

[18]Z. Chen and S. Rhee, "Effect of traveling wave on the vortex-induced vibration of a long flexible pipe," Appl. Ocean Res. **84**, 122–132 (2019).

[19]J. K. Vandiver, V. Jaiswal, and V. Jhingran, "Insights on vortex-induced, traveling waves on long risers," J. Fluids Struct. **25**, 641–653 (2009).

[20]J. K. Vandiver, L. Ma, and Z. Rao, "Revealing the effects of damping on the flow-induced vibration of flexible cylinders," J. Sound Vib. **433**, 29–54 (2018).

[21]D. Fan, Z. Wang, M. S. Triantafyllou, and G. E. Karniadakis, "Mapping the properties of the vortex-induced vibrations of flexible cylinders in uniform oncoming flow," J. Fluid Mech. **881**, 815–858 (2019).

[22]P. Voie, J. Wu, T. L. Resvanis, C. M. Larsen, J. K. Vandiver, M. S. Triantafyllou, and R. Baarholm, "Consolidation of empirics for calculation of VIV response," in *Proceedings of the 24th International Conference on Offshore Mechanics and Arctic Engineering* (American Society of Mechanical Engineers, 2017), Vol. 57649.

[23]M. S. Triantafyllou, G. S. Triantafyllou, Y. S. Tein, and B. D. Ambrose, "Pragmatic riser VIV analysis," in Offshore Technology Conference (1999).

[24]C. M. Larsen, K. Vikestad, R. Yttervik, E. Passano, and G. S. Baarholm, *Vivana Theory Manual* (Marintek, Trondheim, Norway, 2001).

[25]J. R. Chaplin, P. W. Bearman, Y. Cheng, E. Fontaine, J. M. R. Graham, K. Herfjord, F. J. Huera-Huarte, M. Isherwood, K. Lambrakos, C. M. Larsen *et al.*, "Blind predictions of laboratory measurements of vortex-induced vibrations of a tension riser," J. Fluids Struct. **21**, 25–40 (2005).

[26]M. I. Jordan and T. M. Mitchell, "Machine learning: Trends, perspectives, and prospects," Science **349**, 255–260 (2015).

[27]D. Silver, J. Schrittwieser, K. Simonyan, I. Antonoglou, A. Huang, A. Guez, T. Hubert, L. Baker, M. Lai, A. Bolton *et al.*, "Mastering the game of go without human knowledge," Nature **550**, 354–359 (2017).

[28]J. Jumper, R. Evans, A. Pritzel, T. Green, M. Figurnov, O. Ronneberger, K. Tunyasuvunakool, R. Bates, A. Žídek, A. Potapenko *et al.*, "Highly accurate protein structure prediction with alphafold," Nature **596**, 583–589 (2021).

[29]G. Chandrashekar and F. Sahin, "A survey on feature selection methods," Comput. Electr. Eng. **40**, 16–28 (2014).

[30]J. Wang, J. Wu, and H. Xiao, "Physics-informed machine learning approach for reconstructing Reynolds stress modeling discrepancies based on DNS data," Phys. Rev. Fluids **2**, 034603 (2017).

[31]M. Raissi, P. Perdikaris, and G. E. Karniadakis, "Physics-informed neural networks: A deep learning framework for solving forward and inverse problems involving nonlinear partial differential equations," J. Comput. Phys. **378**, 686–707 (2019).

[32]M. Raissi, A. Yazdani, and G. E. Karniadakis, "Hidden fluid mechanics: Learning velocity and pressure fields from flow visualizations," Science **367**, 1026–1030 (2020).

[33]C. Park, R. T. Haftka, and N. H. Kim, "Remarks on multi-fidelity surrogates," Struct. Multidiscip. Optim. **55**, 1029–1050 (2017).

[34]D. Brika and A. Laneville, "Vortex-induced vibrations of a long flexible circular cylinder," J. Fluid Mech. **250**, 481–508 (1993).

[35]J. R. Chaplin, P. W. Bearman, F. J. Huera-Huarte, and R. J. Pattenden, "Laboratory measurements of vortex-induced vibrations of a vertical tension riser in a stepped current," J. Fluids Struct. **21**, 3–24 (2005).

[36]F. J. Huera-Huarte, "Multi-mode vortex-induced vibrations of a flexible circular cylinder," Ph.D. thesis (University of London, 2006).

[37]F. J. Huera-Huarte and P. W. Bearman, "Wake structures and vortex-induced vibrations of a long flexible cylinder—Part 1: Dynamic response," J. Fluids Struct. **25**, 969–990 (2009).

[38]F. J. Huera-Huarte and P. W. Bearman, "Wake structures and vortex-induced vibrations of a long flexible cylinder–Part 2: Drag coefficients and vortex modes," J. Fluids Struct. **25**, 991–1006 (2009).

[39]C. Grouthier, S. Michelin, Y. Modarres-Sadeghi, and E. de Langre, "Self-similar vortex-induced vibrations of a hanging string," J. Fluid Mech. **724**, R2 (2013).

[40]G. R. Franzini, C. P. Pesce, R. T. Gon ç alves, A. L. C. Fujarra, and P. Mendes, "Experimental investigations on vortex-induced vibrations with a long flexible cylinder. Part I: Modal-amplitude analysis with a vertical configuration," in 11th International Conference on Flow-Induced Vibration (2016).

[41]B. Seyed-Aghazadeh and Y. Modarres-Sadeghi, "Reconstructing the vortex-induced-vibration response of flexible cylinders using limited localized measurement points," J. Fluids Struct. **65**, 433–446 (2016).

[42]E. D. Gedikli and J. M. Dahl, "Mode excitation hysteresis of a flexible cylinder undergoing vortex-induced vibrations," J. Fluids Struct. **69**, 308–322 (2017).

[43]M. A. Tognarelli, S. T. Slocum, W. R. Frank, and R. B. Campbell, "Viv response of a long flexible cylinder in uniform and linearly sheared currents," in *Offshore Technology Conference* (OnePetro, 2004).

[44]A. D. Trim, H. Braaten, H. Lie, and M. A. Tognarelli, "Experimental investigation of vortex-induced vibration of long marine risers," J. Fluids Struct. **21**, 335–361 (2005).

[45]Y. Modarres-Sadeghi, H. Mukundan, J. M. Dahl, F. S. Hover, and M. S. Triantafyllou, "The effect of higher harmonic forces on fatigue life of marine risers," J. Sound Vib. **329**, 43–55 (2010).

[46]Y. Modarres-Sadeghi, F. Chasparis, M. S. Triantafyllou, M. Tognarelli, and P. Beynet, "Chaotic response is a generic feature of vortex-induced vibrations of flexible risers," J. Sound Vib. **330**, 2565–2579 (2011).

[47]Y. Gao, S. Fu, J. Wang, L. Song, and Y. Chen, "Experimental study of the effects of surface roughness on the vortex-induced vibration response of a flexible cylinder," Ocean Eng. **103**, 40–54 (2015).

[48]Y. Gao, S. Fu, Y. Xiong, Y. Zhao, and L. Liu, "Experimental study on response performance of vortex-induced vibration on a flexible cylinder," Ships Offshore Struct. **12**, 116–134 (2017).

[49]M. L. Facchinetti, E. De Langre, and F. Biolley, "Coupling of structure and wake oscillators in vortex-induced vibrations," J. Fluids Struct. **19**, 123–140 (2004).

[50]R. Violette, E. De Langre, and J. Szydlowski, "Computation of vortex-induced vibrations of long structures using a wake oscillator model: Comparison with DNS and experiments," Comput. Struct. **85**, 1134–1141 (2007).

[51]N. Srinil and H. Zanganeh, "Modelling of coupled cross-flow/in-line vortex-induced vibrations using double duffing and van der pol oscillators," Ocean Eng. **53**, 83–97 (2012).

[52]N. Srinil, P. A. Opinel, and F. Tagliaferri, "Empirical sensitivity of two-dimensional nonlinear wake–cylinder oscillators in cross-flow/in-line vortex-induced vibrations," J. Fluids Struct. **83**, 310–338 (2018).

[53]D. J. Newman and G. E. Karniadakis, "A direct numerical simulation study of flow past a freely vibrating cable," J. Fluid Mech. **344**, 95–136 (1997).

[54]C. Evangelinos and G. E. Karniadakis, "Dynamics and flow structures in the turbulent wake of rigid and flexible cylinders subject to vortex-induced vibrations," J. Fluid Mech. **400**, 91–124 (1999).

[55]Y. Bao, R. Palacios, M. Graham, and S. Sherwin, "Generalized thick strip modelling for vortex-induced vibration of long flexible cylinders," J. Comput. Phys. **321**, 1079–1097 (2016).

[56]Y. Bao, H. Zhu, P. Huan, R. Wang, D. Zhou, Z. Han, R. Palacios, M. Graham, and S. Sherwin, "Numerical prediction of vortex-induced vibration of flexible riser with thick strip method," J. Fluids Struct. **89**, 166–173 (2019).

[57]K. Lin and J. Wang, "Numerical simulation of vortex-induced vibration of long flexible risers using a SDVM-FEM coupled method," Ocean Eng. **172**, 468–486 (2019).

[58] H. Zheng and J. Wang, "A numerical study on the vortex-induced vibration of flexible cylinders covered with differently placed buoyancy modules," J. Fluids Struct. **100**, 103174 (2021).

[59] K. Lin, D. Fan, and J. Wang, "Dynamic response and hydrodynamic coefficients of a cylinder oscillating in crossflow with an upstream wake interference," Ocean Eng. **209**, 107520 (2020).

[60] K. Raghavan and M. M. Bernitsas, "Experimental investigation of reynolds number effect on vortex induced vibration of rigid circular cylinder on elastic supports," Ocean Eng. **38**, 719–731 (2011).

[61] Y. Wang, D. Gao, and J. Fang, "Coupled dynamic analysis of deepwater drilling riser under combined forcing and parametric excitation," J. Nat. Gas Sci. Eng. **27**, 1739–1747 (2015).

[62] G. Riches, R. Martinuzzi, and C. Morton, "Proper orthogonal decomposition analysis of a circular cylinder undergoing vortex-induced vibrations," Phys. Fluids **30**, 105103 (2018).

[63] R. Bourguet, G. E. Karniadakis, and M. S. Triantafyllou, "Distributed lock-in drives broadband vortex-induced vibrations of a long flexible cylinder in shear flow," J. Fluid Mech. **717**, 361–375 (2013).

[64] N. Jauvtis and C. H. K. Williamson, "The effect of two degrees of freedom on vortex-induced vibration at low mass and damping," J. Fluid Mech. **509**, 23–62 (2004).

[65] H. Zheng, J. M. Dahl, Y. Modarres-Sadeghi, and M. S. Triantafyllou, "Coupled inline-cross flow vortex-induced vibration hydrodynamic coefficients database," in *Proceedings of the 33th OMAE Conference* (American Society of Mechanical Engineers, 2014).

[66] D. Fan and M. S. Triantafyllou, "Vortex-induced vibration of riser with low span to diameter ratio buoyancy modules," in *The 27th International Ocean and Polar Engineering Conference* (International Society of Offshore and Polar Engineers, 2017).

[67] H. Braaten and H. Lie, "NDP riser high mode VIV tests," Report No. 512394.00.01 (Norwegian Marine Technology Research Institute, 2004).

[68] Z. Wang, D. Fan, and M. S. Triantafyllou, "Illuminating the complex role of the added mass during vortex induced vibration," Phys. Fluids **33**, 085120 (2021).

[69] J. K. Vandiver, "Drag coefficients of long flexible cylinders," in *Offshore Technology Conference* (OnePetro, 1983).

[70] J. K. Vandiver and J. Jong, "The relationship between in-line and cross-flow vortex-induced vibration of cylinders," J. Fluids Struct. **1**, 381–399 (1987).

[71] R. Bruschi, G. Buresti, A. Castoldi, and E. Migliavacca, "Vortex shedding oscillations for submarine pipelines: Comparison between full-scale experiments and analytical models," in *14th Offshore Technology Conference* (Offshore Technology Conference, 1982), Vol. 4232.

[72] F. Webster, "Vertical profiles of horizontal ocean currents," Deep Sea Res. Oceanogr. Abstr. **16**, 85–98 (1969).

[73] F. Rowe and J. Young, "An ocean current profiler using Doppler sonar," in *OCEANS'79* (IEEE, 1979), pp. 292–297.

[74] Y. Kim, J. K. Vandiver, and R. Holler, "Vortex-induced vibration and drag coefficients of long cables subjected to sheared flows," J. Energy Resour. Technol. **108**, 77–83 (1986).

[75] J. K. Vandiver and A. Marcollo, "High mode number VIV experiments," in *IUTAM Symposium on Integrated Modeling of Fully Coupled Fluid Structure Interactions Using Analysis, Computations and Experiments: Proceedings of the IUTAM Symposium* (Springer, 2003), pp. 211–231.

[76] J. K. Vandiver, H. Marcollo, S. Swithenbank, and V. Jhingran, "High mode number vortex-induced vibration field experiments," in *Offshore Technology Conference* (OnePetro, 2005).

[77] J. K. Vandiver, S. B. Swithenbank, V. Jaiswal, and V. Jhingran, "Fatigue damage from high mode number vortex-induced vibration," in Proceedings of the 25th OMAE Conference (2006).

[78] H. Marcollo, H. Chaurasia, and J. K. Vandiver, "Phenomena observed in VIV bare riser field tests," in *International Conference on Offshore Mechanics and Arctic Engineering* (ASME, OMAE, 2007), Vol. 4269, pp. 989–995.

[79] P. K. Stansby, "The locking-on of vortex shedding due to the cross-stream vibration of circular cylinders in uniform and shear flows," J. Fluid Mech. **74**, 641–665 (1976).

[80] D. Allen, E. Dension, and J. Bos, "Vortex-induced vibration of cylindrical structures in sheared flow" (Shell and MIT, 1992).

[81] H. Lie, K. Mo, and J. K. Vandiver, "VIV model test of a bare-and a staggered buoyancy riser in a rotating rig," in *Offshore Technology Conference* (OnePetro, 1998).

[82] D. Lucor, L. Imas, and G. E. Karniadakis, "Vortex dislocations and force distribution of long flexible cylinders subjected to sheared flows," J. Fluids Struct. **15**, 641–650 (2001).

[83] N. Srinil, "Multi-mode interactions in vortex-induced vibrations of flexible curved/straight structures with geometric nonlinearities," J. Fluids Struct. **26**, 1098–1122 (2010).

[84] N. Srinil, "Analysis and prediction of vortex-induced vibrations of variable-tension vertical risers in linearly sheared currents," Appl. Ocean Res. **33**, 41–53 (2011).

[85] R. Bourguet, G. E. Karniadakis, and M. S. Triantafyllou, "Vortex-induced vibrations of a long flexible cylinder in shear flow," J. Fluid Mech. **677**, 342–382 (2011).

[86] R. Bourguet, G. E. Karniadakis, and M. S. Triantafyllou, "Multi-frequency vortex-induced vibrations of a long tensioned beam in linear and exponential shear flows," J. Fluids Struct. **41**, 33–42 (2013).

[87] P. W. Bearman, M. J. Downie, J. M. R. Graham, and E. D. Obasaju, "Forces on cylinders in viscous oscillatory flow at low Keulegan-Carpenter numbers," J. Fluid Mech. **154**, 337–356 (1985).

[88] C. H. K. Williamson, "Fluid forces on a small cylinder in the presence of a large cylinder in relative oscillatory flow," Appl. Ocean Res. **7**, 124–127 (1985).

[89] T. Sarpkaya, "Force on a circular cylinder in viscous oscillatory flow at low Keulegan–Carpenter numbers," J. Fluid Mech. **165**, 61–71 (1986).

[90] D. Fan, X. Zhang, M. S. Triantafyllou *et al.*, "Drag coefficient enhancement of dual cylinders in oscillatory flow," in *The 27th International Ocean and Polar Engineering Conference* (International Society of Offshore and Polar Engineers, 2017).

[91] D. Zhang, Xa Fan, D. Wan *et al.*, "Numerical study of oscillatory dual cylinders in tandem arrangement," in Proceedings of the Twenty-Seventh (2017) International Ocean and Polar Engineering Conference San Francisco, CA (2017).

[92] S. Fu, J. Wang, R. Baarholm, J. Wu, and C. M. Larsen, "Features of vortex-induced vibration in oscillatory flow," J. Offshore Mech. Arct. Eng. **136**, 011801 (2014).

[93] J. Wang, S. Xiang, S. Fu, P. Cao, J. Yang, and J. He, "Experimental investigation on the dynamic responses of a free-hanging water intake riser under vessel motion," Mar. Struct. **50**, 1–19 (2016).

[94] J. Wang, S. Fu, J. Wang, H. Li, and M. C. Ong, "Experimental investigation on vortex-induced vibration of a free-hanging riser under vessel motion and uniform current," J. Offshore Mech. Arct. Eng. **139**(4), 041703 (2017).

[95] T. L. Resvanis, "Vortex-induced vibration of flexible cylinders in time-varying flows," Ph.D. thesis (Massachusetts Institute of Technology, 2014).

[96] C. H. K. Williamson, "Vortex dynamics in the cylinder wake," Annu. Rev. Fluid Mech. **28**, 477–539 (1996).

[97] M. J. Thorsen, S. Sævik, and C. M. Larsen, "Time domain simulation of vortex-induced vibrations in stationary and oscillating flows," J. Fluids Struct. **61**, 1–19 (2016).

[98] J. V. Ulveseter, M. J. Thorsen, S. Sævik, and C. M. Larsen, "Time domain simulation of riser VIV in current and irregular waves," Mar. Struct. **60**, 241–260 (2018).

[99] Z. Lu, S. Fu, M. Zhang, and H. Ren, "An efficient time-domain prediction model for vortex-induced vibration of flexible risers under unsteady flows," Mar. Struct. **64**, 492–519 (2019).

[100] W. Xu, Y. Ma, C. Ji, and C. Sun, "Laboratory measurements of vortex-induced vibrations of a yawed flexible cylinder at different yaw angles," Ocean Eng. **154**, 27–42 (2018).

[101] W. Xu, Y. Luan, Q. Han, C. Ji, and A. Cheng, "The effect of yaw angle on VIV suppression for an inclined flexible cylinder fitted with helical strakes," Appl. Ocean Res. **67**, 263–276 (2017).

[102] L. Ma, "Using superposition of undamped modes to model non-orthogonally damped systems," Ph.D. thesis (Massachusetts Institute of Technology, 2017).

[103] L. Ma, T. L. Resvanis, and J. K. Vandiver, "Using machine learning to identify important parameters for flow-induced vibration," in *International

Conference on Offshore Mechanics and Arctic Engineering (American Society of Mechanical Engineers, 2020), Vol. 84355.

[104]L. Ma, "Understanding flow-induced vibration via a physics-constrained, data-driven approach," Ph.D. thesis (Massachusetts Institute of Technology, 2021).

[105]Z. Wang, D. Fan, M. S. Triantafyllou, and G. E. Karniadakis, "A large-eddy simulation study on the similarity between free vibrations of a flexible cylinder and forced vibrations of a rigid cylinder," J. Fluids Struct. **101**, 103223 (2021).

[106]Y. Chen, S. Fu, Y. Xu, and D. Fan, "High order force components of a near-wall circular cylinder oscillating in transverse direction in a steady current," Ocean Eng. **74**, 37–47 (2013).

[107]J. L. Garrec, D. Fan, B. Wu, and M. S. Triantafyllou, "Experimental investigation of cross flow-inline coupled vortex-induced vibration on riser with finite length buoyancy module," in *OCEANS 2016 MTS/IEEE Monterey* (IEEE, 2016), pp. 1–7.

[108]B. Wu, J. L. Garrec, D. Fan, and M. S. Triantafyllou, "Kill line model cross flow inline coupled vortex-induced vibration," in *Proceedings of the 36th OMAE Conference* (American Society of Mechanical Engineers, 2017), Vol. 57649.

[109]F. J. Huera-Huarte, P. W. Bearman, and J. R. Chaplin, "On the force distribution along the axis of a flexible circular cylinder undergoing multi-mode vortex-induced vibrations," J. Fluids Struct. **22**, 897–903 (2006).

[110]G. Tang, L. Lu, B. Teng, H. Park, J. Song, and J. Zhang, "Identification of hydrodynamic coefficients from experiment of vortex-induced vibration of slender riser model," Sci. China Technol. Sci. **54**, 1894–1905 (2011).

[111]J. Wu, "Hydrodynamic force identification from stochastic vortex induced vibration experiments with slender beams," Ph.D. thesis (Norwegian University of Science and Technology, 2011).

[112]L. Song, S. Fu, J. Cao, L. Ma, and J. Wu, "An investigation into the hydrodynamics of a flexible riser undergoing vortex-induced vibration," J. Fluids Struct. **63**, 325–350 (2016).

[113]Q. Han, Y. Ma, W. Xu, D. Fan, and E. Wang, "Hydrodynamic characteristics of an inclined slender flexible cylinder subjected to vortex-induced vibration," Inter. J. Mech. Sci. **148**, 352–365 (2018).

[114]Z. Rao, T. L. Resvanis, and J. K. Vandiver, "The identification of power-in region in vortex-induced vibration of flexible cylinders," in *Proceedings of the 33th OMAE Conference* (American Society of Mechanical Engineers, 2014), Vol. 45400

[115]D. Fan, L. Yang, Z. Wang, M. S. Triantafyllou, and G. E. Karniadakis, "Reinforcement learning for bluff body active flow control in experiments and simulations," Proc. Natl. Acad. U. S. A. **117**, 26091–26098 (2020).

[116]D. Fan, G. Jodin, T. R. Consi, L. Bonfiglio, Y. Ma, L. R. Keyes, G. E. Karniadakis, and M. S. Triantafyllou, "A robotic intelligent towing tank for learning complex fluid-structure dynamics," Sci. Rob. **4**, eaay5063 (2019).

[117]R. Bourguet, Y. Modarres-Sadeghi, G. E. Karniadakis, and M. S. Triantafyllou, "Wake-body resonance of long flexible structures is dominated by counter-clockwise orbits," Phys. Rev. Lett. **107**, 134502 (2011).

[118]Z. A. Bangash and F. J. Huera-Huarte, "On the flow around the node to anti-node transition of a flexible cylinder undergoing vortex-induced vibrations," Phys. Fluids **27**, 065112 (2015).

[119]H. Zhu, D. Zhou, Y. Bao, R. Wang, J. Lu, D. Fan, and Z. Han, "Wake characteristics of stationary catenary risers with different incoming flow directions," Ocean Eng. **167**, 142–155 (2018).

[120]Z. Zhang, C. Ji, M. M. Alam, and D. Xu, "Dns of vortex-induced vibrations of a yawed flexible cylinder near a plane boundary," Wind Struct. **30**, 465–474 (2020).

[121]C. Ji, Z. Peng, M. M. Alam, W. Chen, D. Xu *et al.*, "Vortex-induced vibration of a long flexible cylinder in uniform cross-flow," Wind Struct. **26**, 267–277 (2018).

[122]Z. Zhang, C. Ji, and D. Xu, "Temporal and spatial evolution of vortex shedding for flow around a cylinder close to a wall," Ocean Eng. **228**, 108964 (2021).

[123]Z. Zhang, C. Ji, W. Chen, Y. Hua, and N. Srinil, "Influence of boundary layer thickness and gap ratios on three-dimensional flow characteristics around a circular cylinder in proximity to a bottom plane," Ocean Eng. **226**, 108858 (2021).

[124]C. Ji, Z. Zhang, D. Xu, and N. Srinil, "Direct numerical simulations of horizontally oblique flows past three-dimensional circular cylinder near a plane boundary," J. Offshore Mech. Arct. Eng. **142**(5), 051903 (2020).

[125]S. Zhao, C. Ji, Z. Sun, H. Yu, and Z. Zhang, "Effect of the yaw angle and spanning length on flow characteristics around a near-wall cylindrical structure," Ocean Eng. **235**, 109340 (2021).

[126]R. Bourguet, G. E. Karniadakis, and M. S. Triantafyllou, "On the validity of the independence principle applied to the vortex-induced vibrations of a flexible cylinder inclined at 60," J. Fluids Struct. **53**, 58–69 (2015).

[127]C. Scruton, "Wind-excited oscillations of tall stacks," Engineer **199**, 806–808 (1955).

[128]R. N. Govardhan and C. H. K. Williamson, "Defining the 'modified griffin plot' in vortex-induced vibration: Revealing the effect of Reynolds number using controlled damping," J. Fluid Mech. **561**, 147–180 (2006).

[129]H. Marcollo, T. Resvanis, C. Dillon, A. Kilner, and J. Vandiver, *Shear7 v4.10 User Guide* (Massachusetts Institute of Technology, Cambridge, MA, 2018).

[130]J. K. Vandiver and L. Ma, "Does more tension reduce VIV?" in *International Conference on Offshore Mechanics and Arctic Engineering* (American Society of Mechanical Engineers, 2017), Vol. 57700.

[131]Y. Kim, "Vortex-induced responses and drag coefficients of long cables in ocean current," Ph.D. thesis (Massachusetts Institute of Technology, 1985).

[132]J. Wu, D. Yin, H. Lie, S. Riemer-Sørensen, S. Sævik, and M. S. Triantafyllou, "Improved VIV response prediction using adaptive parameters and data clustering," J. Mar. Sci. Eng. **8**, 127 (2020).

[133]B. Seyed-Aghazadeh, M. Edraki, and Y. Modarres-Sadeghi, "Effects of boundary conditions on vortex-induced vibration of a fully submerged flexible cylinder," Exp. Fluids **60**, 38 (2019).

[134]C. Grouthier, S. Michelin, R. Bourguet, Y. Modarres-Sadeghi, and E. De Langre, "On the efficiency of energy harvesting using vortex-induced vibrations of cables," J. Fluids Struct. **49**, 427–440 (2014).

[135]G. R. S. Assi, P. W. Bearman, and J. R. Meneghini, "On the wake-induced vibration of tandem circular cylinders: The vortex interaction excitation mechanism," J. Fluid Mech. **661**, 365–401 (2010).

[136]J. Wang and D. Fan, "An active learning strategy to study the flow control of a stationary cylinder with two asymmetrically attached rotating cylinders," in *The 30th ISOPE Conference* (OnePetro, 2020).

[137]D. Fan, L. Yang, Z. Wang, M. S. Triantafyllou, and G. E. Karniadakis, "Deep reinforcement learning for bluff body active flow control in experiments and simulations," in APS Division of Fluid Dynamics Meeting Abstracts (2020).

[138]M. M. Zdravkovich, "Review of interference-induced oscillations in flow past two parallel circular cylinders in various arrangements," J. Wind. Eng. Ind. **28**, 183–199 (1988).

[139]F. J. Huera-Huarte and P. W. Bearman, "Vortex and wake-induced vibrations of a tandem arrangement of two flexible circular cylinders with near wake interference," J. Fluids Struct. **27**, 193–211 (2011).

[140]F. J. Huera-Huarte and M. Gharib, "Vortex-and wake-induced vibrations of a tandem arrangement of two flexible circular cylinders with far wake interference," J. Fluids Struct. **27**, 824–828 (2011).

[141]W. Xu, Y. Ma, A. Cheng, and H. Yuan, "Experimental investigation on multi-mode flow-induced vibrations of two long flexible cylinders in a tandem arrangement," Int. J. Mech. Sci. **135**, 261–278 (2018).

[142]W. Xu, Y. Li, W. Ma, K. Liang, and Y. Yu, "Effects of spacing ratio on the fiv fatigue damage characteristics of a pair of tandem flexible cylinders," Appl. Ocean Res. **102**, 102299 (2020).

[143]A. Bokaian and F. Geoola, "Wake-induced galloping of two interfering circular cylinders," J. Fluid Mech. **146**, 383–415 (1984).

[144]F. S. Hover and M. S. Triantafyllou, "Galloping response of a cylinder with upstream wake interference," J. Fluids Struct. **15**, 503–512 (2001).

[145]G. R. S. Assi, P. W. Bearman, B. S. Carmo, J. R. Meneghini, S. J. Sherwin, and R. H. J. Willden, "The role of wake stiffness on the wake-induced vibration of the downstream cylinder of a tandem pair," J. Fluid Mech. **718**, 210–245 (2013).

[146]H. Jing, F. Huang, X. He, and C. Cai, "Wake-induced vibrations of tandem flexible cable models in a wind tunnel," Ocean Eng. **233**, 109188 (2021).

[147]R. King and D. J. Johns, "Wake interaction experiments with two flexible circular cylinders in flowing water," J. Sound Vib. **45**, 259–283 (1976).

[148]K. Lin, J. Wang, D. Fan, and M. S. Triantafyllou, "Flow-induced cross-flow vibrations of long flexible cylinder with an upstream wake interference," Phys. Fluids **33**, 065104 (2021).

[149] D. W. Allen and D. L. Henning, "Vortex-induced vibration current tank tests of two equal-diameter cylinders in tandem," J. Fluids Struct. **17**, 767–781 (2003).

[150] F. J. Huera-Huarte, Z. A. Bangash, and L. M. González, "Multi-mode vortex and wake-induced vibrations of a flexible cylinder in tandem arrangement," J. Fluids Struct. **66**, 571–588 (2016).

[151] H. Liu, F. Wang, G. Jiang, X. Guo, and H. Li, "Laboratory measurements of vortex-and wake-induced vibrations of a tandem arrangement of two flexible risers," China Ocean Eng. **30**, 47–56 (2016).

[152] B. Seyed-Aghazadeh, N. Anderson, and S. Dulac, "Flow-induced vibration of high-mass ratio isolated and tandem flexible cylinders with fixed boundary conditions," J. Fluids Struct. **103**, 103276 (2021).

[153] P. Jiang, Z. Li, L. Feng, Y. Wang, L. Liu, and H. Guo, "Experimental investigation on the VIV of two side-by-side risers fitted with triple helical strakes under coupled interference effect," J. Fluids Struct. **101**, 103202 (2021).

[154] F. J. Huera-Huarte and M. Gharib, "Flow-induced vibrations of a side-by-side arrangement of two flexible circular cylinders," J. Fluids Struct. **27**, 354–366 (2011).

[155] B. Sanaati and N. Kato, "A study on the proximity interference and synchronization between two side-by-side flexible cylinders," Ocean Eng. **85**, 65–79 (2014).

[156] W. Xu, Y. Li, K. Jia, and Y. Yu, "Fiv induced fatigue damage of two side-by-side flexible cylinders in a uniform flow," Ocean Eng. **217**, 107898 (2020).

[157] D. Brika and A. Laneville, "The flow interaction between a stationary cylinder and a downstream flexible cylinder," J. Fluids Struct. **13**, 579–606 (1999).

[158] W. Xu, A. Cheng, Y. Ma, and X. Gao, "Multi-mode flow-induced vibrations of two side-by-side slender flexible cylinders in a uniform flow," Mar. Struct. **57**, 219–236 (2018).

[159] W. Xu, W. Qin, and Y. Yu, "Flow-induced vibration of two identical long flexible cylinders in a staggered arrangement," Int. J. Mech. Sci. **180**, 105637 (2020).

[160] W. Xu, Q. Zhang, J. Lai, Q. Wang, and Y. Yu, "Flow-induced vibration of two staggered flexible cylinders with unequal diameters," Ocean Eng. **211**, 107523 (2020).

[161] Q. Han, Y. Ma, W. Xu, and S. Zhang, "An experimental study on the hydrodynamic features of two side-by-side flexible cylinders undergoing flow-induced vibrations in a uniform flow," Mar. Struct. **61**, 326–342 (2018).

[162] E. Wang, Q. Xiao, Q. Zhu, and A. Incecik, "The effect of spacing on the vortex-induced vibrations of two tandem flexible cylinders," Phys. Fluids **29**, 077103 (2017).

[163] H. Chen, C. Chen, and K. Huang, "CFD simulation of vortex-induced and wake-induced vibrations of dual vertical risers," in The 23rd *ISOPE Conference* (OnePetro, 2013).

[164] A. Krizhevsky, I. Sutskever, and G. E. Hinton, "Imagenet classification with deep convolutional neural networks," Adv. Neural Inf. Process. Syst. **25**, 1097–1105 (2012).

[165] K. R. Chowdhary, "Natural language processing," *Fundamentals Artificial Intelligence* (Springer Nature, 2020), pp. 603–649.

[166] O. Vinyals, I. Babuschkin, W. M. Czarnecki, M. Mathieu, A. Dudzik, J. Chung, D. H. Choi, R. Powell, T. Ewalds, P. Georgiev *et al.*, "Grandmaster level in Starcraft II using multi-agent reinforcement learning," Nature **575**, 350–354 (2019).

[167] S. L. Brunton, B. R. Noack, and P. Koumoutsakos, "Machine learning for fluid mechanics," Annu. Rev. Fluid Mech. **52**, 477–508 (2020).

[168] M. P. Brenner, J. D. Eldredge, and J. B. Freund, "Perspective on machine learning for advancing fluid mechanics," Phys. Rev. Fluids **4**, 100501 (2019).

[169] K. Fukami, K. Fukagata, and K. Taira, "Assessment of supervised machine learning methods for fluid flows," Theor. Comput. Fluid. Dyn. **34**, 497–519 (2020).

[170] F. Ren, C. Wang, and H. Tang, "Active control of vortex-induced vibration of a circular cylinder using machine learning," Phys. Fluids **31**, 093601 (2019).

[171] F. Ren, C. Wang, and H. Tang, "Bluff body uses deep-reinforcement-learning trained active flow control to achieve hydrodynamic stealth," Phys. Fluids **33**, 093602 (2021).

[172] Y.-F. Mei, C. Zheng, N. Aubry, M.-G. Li, W.-T. Wu, and X. Liu, "Active control for enhancing vortex induced vibration of a circular cylinder based on deep reinforcement learning," Phys. Fluids **33**, 103604 (2021).

[173] S. Li, S. Laima, and H. Li, "Physics-guided deep learning framework for predictive modeling of bridge vortex-induced vibrations from field monitoring," Phys. Fluids **33**, 037113 (2021).

[174] S. H. Rudy, S. L. Brunton, J. L. Proctor, and J. N. Kutz, "Data-driven discovery of partial differential equations," Sci. Adv. **3**, e1602614 (2017).

[175] S. Li, E. Kaiser, S. Laima, H. Li, S. L. Brunton, and J. N. Kutz, "Discovering time-varying aerodynamics of a prototype bridge by sparse identification of nonlinear dynamical systems," Phys. Rev. E **100**, 022220 (2019).

[176] L. Ma, T. L. Resvanis, and J. K. Vandiver, "A weighted sparse-input neural network technique applied to identify important features for vortex-induced vibration," in *AAAI Spring Symposium: MLPS* (AAAI, 2020).

[177] L. Ma, "Interpretable machine learning for insight extraction from rigid cylinder flow-induced vibration phenomena," Appl. Ocean Res. **119**, 102975 (2022).

[178] L. Ma, T. L. Resvanis, and J. K. Vandiver, "Enhancing machine learning models with prior physical knowledge to aid in VIV response prediction," in *International Conference on Offshore Mechanics and Arctic Engineering* (American Society of Mechanical Engineers, 2021).

[179] S. Riemer-Sørensen, J. Wu, H. Lie, S. Sævik, and S. W. Kim, "Data-driven prediction of vortex-induced vibration response of marine risers subjected to three-dimensional current," in *Symposium of the Norwegian AI Society* (Springer, 2019), pp. 78–89.

[180] M. Apolinario and R. Coutinho, "Understanding the biofouling of offshore and deep-sea structures," in *Advances in Marine Antifouling Coatings and Technologies* (Elsevier, 2009), pp. 132–147.

[181] H. Mukundan, Y. Modarres-Sadeghi, F. S. Dahl, J. M. Hover, and M. S. Triantafyllou, "Monitoring VIV fatigue damage on marine risers," J. Fluids Struct. **25**, 617–628 (2009).

[182] A. C. Phadke, "Marine composite riser for structural health monitoring using piezoelectricity," U.S. patent 8,800,665 (2014).

[183] J. K. Vandiver, "Research challenges in the vortex-induced vibration prediction of marine risers," in *Offshore Technology Conference* (OnePetro, 1998).

[184] S. W. Doebling, C. R. Farrar, M. B. Prime, and D. W. Shevitz, "Damage identification and health monitoring of structural and mechanical systems from changes in their vibration characteristics: A literature review," U.S. Department of Energy Office of Scientific and Technical Information (1996).

[185] W. Staszewski, C. Boller, and G. R. Tomlinson, *Health Monitoring of Aerospace Structures: Smart Sensor Technologies and Signal Processing* (John Wiley & Sons, 2004).

[186] Y. Xu, S. Fu, Q. Zhong, D. Fan, Y. Zhang, and R. Li, "Online safety monitor design of the jacket platform based on structural members failure study," in *International Conference on Offshore Mechanics and Arctic Engineering* (American Society of Mechanical Engineers, 2013), Vol. 55317.

[187] S. Khatir, K. Dekemele, M. Loccufier, T. Khatir, and M. A. Wahab, "Crack identification method in beam-like structures using changes in experimentally measured frequencies and particle swarm optimization," C. R. Méc. **346**, 110–120 (2018).

[188] E. Kharazmi, D. Fan, Z. Wang, and M. S. Triantafyllou, "Inferring vortex induced vibrations of flexible cylinders using physics-informed neural networks," J. Fluids Struct. **107**, 103367 (2021).

[189] Z. Mao, A. D. Jagtap, and G. E. Karniadakis, "Physics-informed neural networks for high-speed flows," Comput. Methods Appl. Mech. Eng. **360**, 112789 (2020).

[190] L. Yang, D. Zhang, and G. E. Karniadakis, "Physics-informed generative adversarial networks for stochastic differential equations," arXiv:1811.02033 (2018).

[191] Y. Yang and P. Perdikaris, "Adversarial uncertainty quantification in physics-informed neural networks," J. Comput. Phys. **394**, 136–152 (2019).

[192] R. Gopalkrishnan, "Vortex-induced forces on oscillating bluff cylinders," Ph. D. thesis (Massachusetts Institute of Technology, 1993).

[193] Y. Xu, S. Fu, Y. Chen, Q. Zhong, and D. Fan, "Experimental investigation on vortex induced forces of oscillating cylinder at high Reynolds number," Ocean Syst. Eng. **3**, 167–180 (2013).

[194] C. J. Chang, R. A. Kumar, and M. M. Bernitsas, "Viv and galloping of single circular cylinder with surface roughness at $3.0 \times 10^4 \leq re \leq 1.2 \times 10^5$," Ocean Eng. **38**, 1713–1732 (2011).

[195] S. Rudy, D. Fan, J. D. A. Ferrandis, T. Sapsis, and M. S. Triantafyllou, "Learning optimal parametric hydrodynamic database for vortex-induced

crossflow vibration prediction of both freely-mounted rigid and flexible cylinders," in *The 31st International Ocean and Polar Engineering Conference* (OnePetro, 2021).

[196]X. Meng, Z. Wang, D. Fan, M. S. Triantafyllou, and G. E. Karniadakis, "A fast multi-fidelity method with uncertainty quantification for complex data correlations: Application to vortex-induced vibrations of marine risers," Comput. Methods Appl. Mech. Eng. **386**, 114212 (2021).

[197]E. Kharazmi, Z. Wang, D. Fan, S. Rudy, T. Sapsis, M. S. Triantafyllou, and G. E. Karniadakis, "From data to assessment models, demonstrated through a digital twin of marine risers," in *Offshore Technology Conference* (OnePetro, 2021).

[198]L. Bonfiglio, P. Perdikaris, S. Brizzolara, and G. E. Karniadakis, "Multi-fidelity optimization of super-cavitating hydrofoils," Comput. Methods Appl. Mech. Eng. **332**, 63–85 (2018).

[199]A. Patra, R. Batra, A. Chandrasekaran, C. Kim, T. D. Huan, and R. Ramprasad, "A multi-fidelity information-fusion approach to machine learn and predict polymer bandgap," Comput. Mater. Sci. **172**, 109286 (2020).

[200]X. Wang, J. Kou, and W. Zhang, "Multi-fidelity surrogate reduced-order modeling of steady flow estimation," Int. J. Numer. Methods Fluids **92**, 1826–1844 (2020).

[201]K. Yoo, O. Bacarreza, and M. F. Aliabadi, "A novel multi-fidelity modelling-based framework for reliability-based design optimisation of composite structures," Eng. Comput. **2020**, 1–14.

[202]T. Lee, I. Bilionis, and A. B. Tepole, "Propagation of uncertainty in the mechanical and biological response of growing tissues using multi-fidelity Gaussian process regression," Comput. Methods Appl. Mech. Eng. **359**, 112724 (2020).

[203]F. S. Costabal, P. Perdikaris, E. Kuhl, and D. E. Hurtado, "Multi-fidelity classification using Gaussian processes: Accelerating the prediction of large-scale computational models," Comput. Methods Appl. Mech. Eng. **357**, 112602 (2019).

[204]Q. Zhou, Y. Wu, Z. Guo, J. Hu, and P. Jin, "A generalized hierarchical co-Kriging model for multi-fidelity data fusion," Struct. Multidiscip. Optim. **62**, 1885–1904 (2020).

[205]K. Tian, Z. Li, L. Huang, K. Du, L. Jiang, and B. Wang, "Enhanced variable-fidelity surrogate-based optimization framework by Gaussian process regression and fuzzy clustering," Comput. Methods Appl. Mech. Eng. **366**, 113045 (2020).

[206]S. Li, W. Xing, R. Kirby, and S. Zhe, "Multi-fidelity Bayesian optimization via deep neural networks," in Advances in Neural Information Processing Systems (2020), Vol. 33.

[207]X. Meng and G. E. Karniadakis, "A composite neural network that learns from multi-fidelity data: Application to function approximation and inverse PDE problems," J. Comput. Phys. **401**, 109020 (2020).

[208]W. Samek, T. Wiegand, and K. R. Müller, "Explainable artificial intelligence: Understanding, visualizing and interpreting deep learning models," arXiv:1708.08296 (2017).